Extrusion of Closed End Tubes for Applications in Sodium-Beta Alumina Solid Electrolytes

Nathan Johnson

Department of Chemical Engineering, University of Birmingham, Edgbaston, B15 2TT

Abstract

The role of efficient energy storage in the distribution of domestic and industrial power is increasing with intermittent renewable energy sources. A method shown to have a low capital cost is the sodium-sulphur battery, which uses a conductive beta-alumina solid electrolyte (BASE) to transfer charge between the anode and cathode. Using paste extrusion to obtain the desired shape, followed by reaction sintering, capital savings could be made compared to the current method of production, electrophoretic deposition. This thesis investigates the role of both solid and liquid components in the paste formulation stage, as well as experimental considerations in the production of the required shape, a hollow tube with one end having a closed, domed shape. It was found that using sources of sodium ions with a high solubility led to undesirable characteristics associated with a change in binder rheology. Predictions for the pressure drop through the die were made with reasonable accuracy, although with such complex geometry, the ram displacement was difficult to predict. Using a die with so many pieces attached together was shown to have difficulties producing a straight extrudate consistently, although the formation of a closed domed end was demonstrated successfully.

Contents

Figures and Tables

1. Introduction

As the global population continues to rise exponentially, so too is the demand for electricity. One thing that is certain not to increase is the amount of resources under the earth's surface, and the global energy landscape is slowly adjusting in response. In addition to changes in supply and demand, it is believed that the combustion of fossil fuels is causing the atmospheric temperature to rise, due to the large amounts of carbon dioxide released. With temperatures set to rise by up to 4^{o}C by 2050 [1], the incentives to move away from the three biggest fossil energy sources, oil, coal and gas, have never been greater.

Vast amounts of money are being spent on new, carbon free energy sources to try and mitigate the effects of climate change. Many of these methods generate electricity from renewable sources, the most adopted methods being wind and solar. These types of energy are referred to as "fluctuating" sources, as their energy output varies depending on environmental conditions. As such, the role of energy storage is becoming more and more important in electricity grids.

Energy storage is one of the great challenges of modern day engineering, as, with such a large focus on efficiency, innovative technologies must do away with the traditional Carnot cycle, which could lose up to 60% of the energy to be stored. One solution is to store the energy by charging a sodium ion battery, which can store energy with a high efficiency for a long period of time. One low cost form of electrochemical storage is the sodium-sulphur battery, a cell with a β-alumina solid electrolyte (BASE) tube which holds molten sodium, and transfers charge to a sulphur cathode. Currently, the solid electrolyte is formed by electrophoretic deposition, but production through extrusion may prove to be an even more cost effective option, lowering the battery cost to a level where it could become a widely used solution for energy storage.

Extrusion is the process by which a paste can be forced under pressure into the shape required for its application. Using this method, it is possible to extrude tubular solid electrolytes for use in energy storage cells. The conductive ceramic allows the transfer of charge between anode and cathode

through mobile ions in the ceramic itself [2]. As such, the electrolyte must not conduct electronically, nor should it allow mixing of the substances at each electrode, achieved by producing a solid with no through-pores.

Consequently, the beta-alumina solid electrolyte (BASE) should resemble a hollow tube, where one end is sealed, allowing separation of the two aqueous electrolytes. In order for the tube to be as strong as possible, it should be formed in one whole piece to prevent weak points where the sealed end is attached. The aim of this project was to develop a method of extruding a paste into this shape, removing the need for a seal to be retrofitted. This process was investigated through a combination of varying paste formulation and rheology, and the use of complex geometries in an extrusion die.

The paste used to make battery cores for such applications contains alpha-alumina, a sodium salt, a source of magnesium atoms such as magnesium oxide, and a binder system. By continuing work previously carried out, both inside and outside the University, a formulation was taken and investigated with regards to the experimental equipment available. The original formulation was found to require extremely high pressures to extrude, and so the rheology of the paste was investigated. Using a simple die, the rheology of similar pastes was quantified according to the parameters expressed in the Benbow-Bridgwater equation [3], which allows predictions to be made about how the paste will behave in an industrial process.

2. Aims and Objectives

- To determine an extrusion process which reliably creates a closed end tube by modification of die configuration.
- To determine the effect of moisture content on the formation of a closed end and subsequent extrusion.
- To determine the effect of chosen sodium salt on the paste rheology.
- To determine the effect of sodium salt on required extrusion pressure.
- To model the extrusion process so as to better predict the effects of formulation on extrusion.

3. Theory, Processes and Materials

The process of producing a product from the extrusion of a paste is well-established, used across a variety of industries, from porcelain, crockery and bricks, to cosmetics, pharmaceutical products and superconductors.

3.1 Newtonian and Non-Newtonian Fluids

In order to effectively investigate the flow of paste through a die in an extrusion process, the rheology of the paste is an important factor, as it determines the pressure required and governs some aspects of die design and apparatus selection.

3.1.1 Newtonian Fluids

Fluids can be classed as being either Newtonian or non-Newtonian, named after physicist Isaac Newton, whose work gave rise to relationships between certain properties of fluids, allowing them to be characterised in this way. A Newtonian fluid is a fluid whose viscosity does not depend on shear rate or shear stress, but on temperature and pressure alone [4]. They are described by:

$$\tau = \eta\dot{\gamma} \qquad (1)$$

where τ is the shear stress, the drag effect on a fluid at the interface with the wall or another phase, η is the fluid viscosity, which is constant for an isothermal system, and $\dot{\gamma}$ is the shear rate, defined as

$$\dot{\gamma} = \frac{d\gamma}{dt} = \frac{\partial v_z}{dr} \qquad (2)$$

for unidirectional flow. This gives a linear relationship between shear stress and shear rate. Fluids which show an “almost” linear relationship between these two properties are said to be Newtonian, examples of which include water and air.

3.1.2 Shear Thinning and Shear Thickening

All fluids which do not fit the Newtonian ideal model are said to be non-Newtonian, where many specific models exist to describe the various different types of non-Newtonian fluids, two of which are shown in Figure .

Shear thinning fluids have a viscosity which decreases as shear stress increases. This is a common characteristic of suspensions, where the decrease in viscosity is due to particles becoming aligned with streamlines in the flow. Alternatively, it may be caused by the breakdown of flocculated particles into smaller units. Shear thickening fluids have a viscosity which increases as the shear stress increases. The increase in viscosity is caused by particles becoming more ordered, or flocculated, and behaving more like a solid.

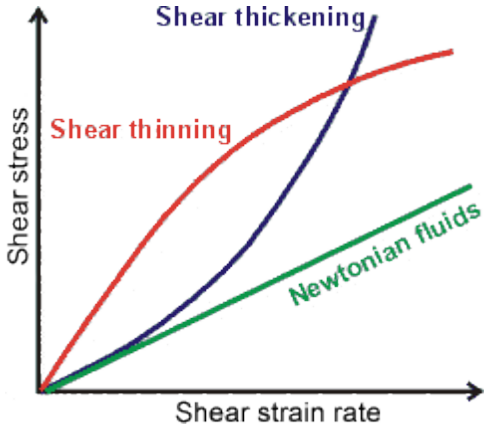

Figure 1 - Diagram to show shear thinning and thickening fluids' behaviour in comparison to Newtonian fluids

For shear thinning and shear thickening fluids, the relationship between shear stress, shear rate and viscosity is described by the Power law

$$\tau = k\dot{\gamma}^{n} \qquad (3)$$

where k is the flow consistency, and n is the flow index. For shear thinning materials, 0 < n < 1, and for shear thickening materials n > 1. By substituting equation 1 into equation 3, the viscosity is given by the equation:

$$\eta = k\dot{\gamma}^{(n-1)} \qquad (4)$$

Some fluids have a viscosity which depends on the duration of the applied shear [5]. In the shear thinning case, these fluids are called thixotropic fluids, where the rate of breakdown of particles into smaller ones is never matched by large particles being reformed, resulting in no equilibrium being

reached. This causes a reversible decrease in viscosity over time. Rheopectic fluids are shear thickening fluids whose viscosity increases with the duration of applied shear. Time dependent shear thickening fluids are extremely rare; the effect is caused by the gradual development of large particles over time, at a faster rate than the breakdown of particles.

3.1.3 Yield Stress

In some cases, particularly concentrated solid suspensions like slurries and pastes, materials will not flow unless a certain threshold of applied force is exceeded. Once this value is exceeded, the material will begin to flow.

A Bingham plastic, named after Eugene Bingham [6], is a material which has a yield stress, below which there is no flow. Once this is exceeded, the material shows a linear relationship between shear stress and strain rate, much like a Newtonian fluid. As such, the plot of shear stress against strain rate resembles that of a Newtonian fluid, but with a positive y-intercept, τ_0, equal to the yield stress. described by the equation

$$\tau = \tau_0 + \eta\dot{\gamma} \quad (5)$$

Another type of fluid to feature a yield stress can be described by the Herschel-Bulkley model, similar to the Bingham plastic model, but featuring the power law model as the second term.

$$\tau = \tau_0 + \eta\dot{\gamma}^n \quad (6)$$

3.2 Paste Formulation and Rheology

The extrusion process uses pressure to form a product from a paste. A paste is a highly concentrated solid suspension, a mixture of solid particles (disperse phase) in a liquid (continuous phase), where the relative amounts of each are chosen such that the material can be easily moulded, but also keeps its shape after processing and produces a product with a high density. The energy

requirements of the process depends heavily on the rheological properties of the paste, which is governed by a number of factors including the ratio of solid and liquid phases, and the interactions between the chemical species present, as well as the rheology of the liquid itself.

3.2.1 Volume and Packing Fraction

The volume fraction of a suspension is defined as the total volume of the solid particles, expressed as a fraction of the volume of both solid and liquid phases, denoted by the symbol ϕ. The addition of solid particles to a liquid will cause the viscosity to increase. This effect is quantified by the Einstein equation, which states that

$$\eta_{rel} = \frac{\eta_{suspension}}{\eta_{liquid}} = 1 + [\eta]\phi \quad (7)$$

where η_{rel} is the ratio of the viscosities of the suspension and liquid phase, and [η] is the intrinsic viscosity, a dimensionless number with a value of 2.5 for rigid, spherical solute particles. This equation is only valid for volume fractions up to 0.1, which makes it unsuitable for use in predicting the viscosity of a paste, a suspension with a much higher fraction of solid particles.

For spherical particles of uniform size, the maximum obtainable volume fraction is 0.64 for a suspension with no applied shear. When shear is applied, this increases to 0.71 as the particles are free to move around. This maximum value is denoted by the symbol ϕ_m, an important value in calculating the viscosity of highly concentrated suspensions. This parameter was used by Krieger and Dougherty in 1959 [7] in calculating the relative viscosity of suspensions with volume fractions higher than anyone had achieved before. The equation they proposed, now referred to as the Krieger-Dougherty equation, is given as

$$\eta_{rel} = \left(1 - \frac{\phi}{\phi_m}\right)^{-[\eta]\phi_m} \quad (8)$$

The maximum packing fraction can be increased by using particles of different sizes, referred to as a polydisperse system. In a bimodal system, a system with two different particle sizes, there exists a higher theoretical limit. In order for the packing fraction to reach this limit, the second set of particles must be sufficiently small to fit in the gaps between the larger particles, usually possible with a size ratio of 7:1 [5]. The value of this maximum can be calculated assuming both particles are spherical, with the equation

$$\phi_{m,bimodal} = \phi_{m,mono} + \left(1 - \phi_{m,mono}\right)\phi_{m,mono} = 0.64 + 0.64(1 - 0.64) = 0.87 \quad (9)$$

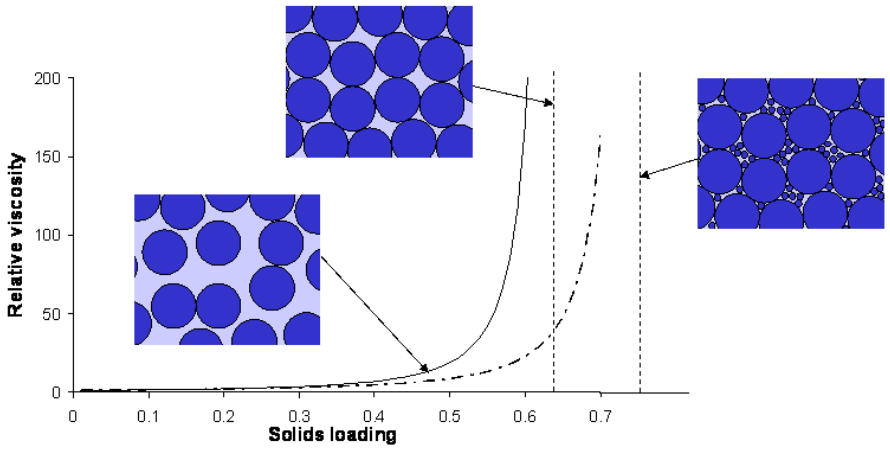

Figure 2 - Graph showing relative viscosity against solids volume fraction for monodisperse and bimodal systems [8]

3.2.2 Liquid Content

As stated previously, the aim of this project is to produce a paste that is easily extrudable, retains its shape after extrusion, and provides a high density product. Although the final product is a solid, liquid is added to aid the shaping process, and removed afterwards. In the absence of enough liquid, gaps will be present between wetted particles, which is a characteristic of a wet powder rather than a paste. A material like this takes a large amount of pressure to shape. Increasing the liquid content past a certain critical value causes a dramatic fall in the material's yield stress, and thus a decrease in the pressure required to shape the material [3].

During the extrusion process, the liquid forms a lubricating layer at the wall, referred to as the "shear zone" [9], with a thickness of a few micrometres. The bulk flow is assumed to move as a plug, with no internal shear, and with a constant velocity across the cross section.

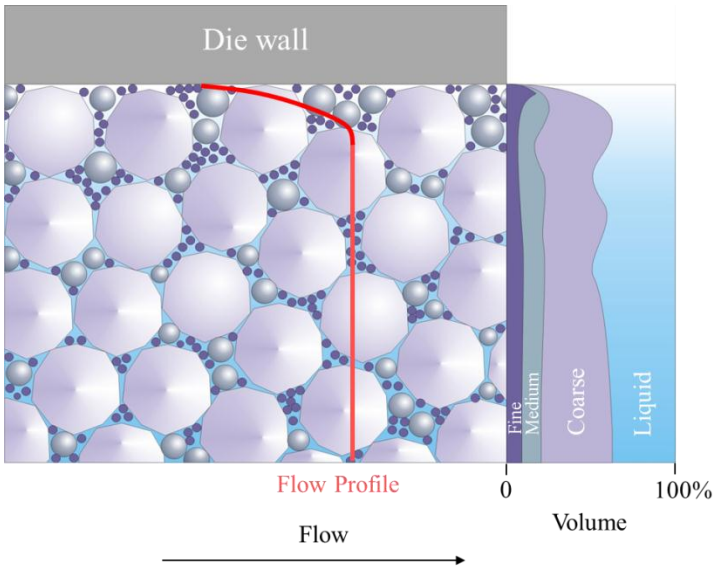

Figure 3 - Diagram of material distribution and velocity profile in paste flow

The liquid layer which forms at the wall can only be formed by excess liquid on top of what is required to fill the voids in the original powder; hence the minimum amount of liquid added to the solid particles must be greater than the total volume of interparticle voids to have an effect on the extrusion pressure.

3.2.3 Organic Binders

One of the key components of a paste is the liquid between the solid particles, for the reasons previously discussed. The liquid used is typically either water or an organic solvent, but in many cases it is beneficial to use water. This is due to its low cost compared to solvents, as well as its inherent safety. This advantage becomes even more significant at the volumes used in industry.

Water alone, however, does not provide the necessary conditions for successful extrusion. It is a Newtonian fluid, with no yield stress, and so the shaped wet ceramic has a low strength. The liquid phase would also be more likely to drain out of the particulate system due to its low viscosity.

Soluble, organic binders are added to the chosen solvent to provide plasticity to the paste, allowing the ceramic to hold its shape before firing [10]. The organic binder changes the behaviour of the liquid in the paste from Newtonian to pseudoplastic, or shear thinning. Once the paste has been extruded, during the drying process, the water evaporates leaving behind the binder, which forms bridges between the particles, giving the ceramic strength, known in this case as green strength.

The majority of prominently used organic binders are long chain polymers, with long chains of covalently bonded carbon atoms, with oxygen, nitrogen and hydrogen atoms attached in large numbers. Also attached to the carbon backbone are side groups, or R groups, whose chemical nature largely determines the solubility of the polymer, and what solvents the polymer will dissolve in. For water, highly polar R-groups promote solubility due to water being a polar solvent. While this match is necessary for dissolution of the solute, it is not sufficient, as the polar R-groups cause interaction between polymer chains, and the solvent must disrupt these interactions in order to dissolve the polymer.

Polymer chains are made up of repeated monomer units. Carbohydrate derived binders feature a ring-type monomer, joined into chains by ether bonds (-O-). The rings are made up of 5 carbon atoms, where R-groups are present on any of the carbon atoms not used to join units together.

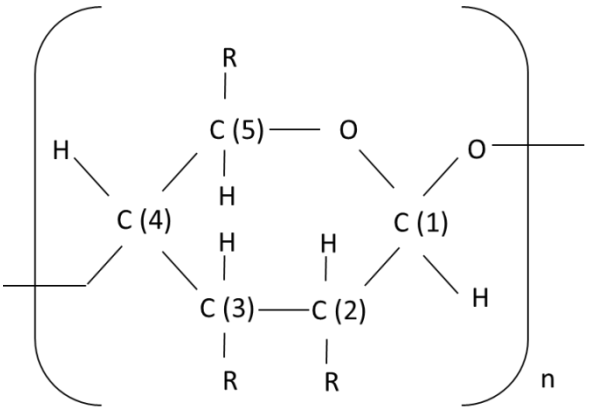

Figure 4 - Modified a-glucose monomer

Figure 4 shows the ring-type monomer present in carbohydrate derived binders, where each carbon atom in the ring is labelled. The degree of polymerisation, n, is the number of monomer units present in a polymer. C-1 and C-4 link the monomers together via ether bonds, while the rest of the carbon atoms are joined to a combination of hydrogen atoms and R-groups. Each binder type has a "degree of substitution", DS, which is the number of R-groups present which are unique to that binder. In the absence of a unique R-group, C-2, C-3 and C-5 are bonded to a hydroxyl group, (-OH). A DS value of one indicates a unique R-group in the C-5 position, while whole number increases fill the C-2 and C-3 positions in that order [10].

Table 1 - Table of water-soluble binders and their R-groups

Binder	R-group	DS
Methylcellulose	$-CH_2-O-CH_3$	2
Hydroxypropylmethylcellulose	$-CH_2-O-CH_2-CH(OH)-CH_3$	2
Hydroxyethylcellulose	$-CH_2-O-C_2H_4-OH$	1
Sodium carboxymethylcellulose	$-CH_2-O-CH_2-COONa$	
Starch	$-CH_2-OH$	
Ammonium alginate	$-COONH_3$	

3.2.4 Paste Flow

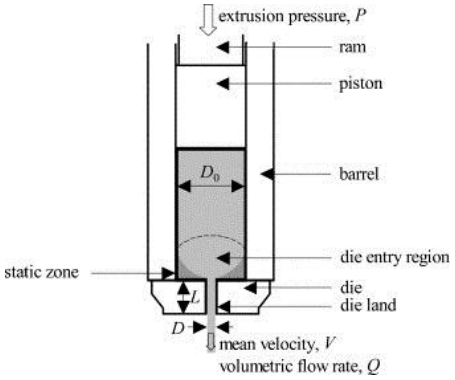

Figure 5 - Diagram of ram extruder with square entry [11]

When a pressure is applied to the ram, it moves towards the die and forces the paste to flow, as in the arrangement shown in Figure 5 - Diagram of ram extruder with square entry. The bulk paste is assumed to move as a plug, with a constant velocity across the channel diameter. Near to the wall exists a high shear region, with a thickness of a few micrometres, where the velocity is lower than that of the bulk , due to the lubrication layer shown in Figure 3.

An important variable, therefore, is the paste velocity, and its relationship with the applied pressure by the ram. The most prevalent method of relating these two variables is the Benbow-Bridgwater equation (20), which provides a way to calculate the pressure drop through a die from a desired extrudate velocity. This equation will be derived in the following few pages.

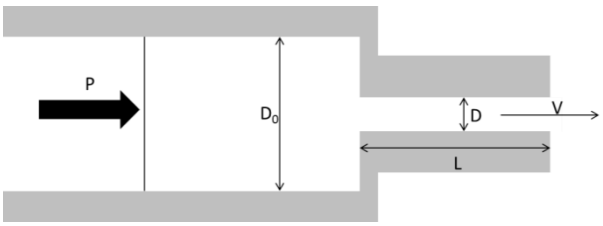

Figure 6 - Diagram of simple square entry extrusion with circular barrel and die land

Figure 6 shows the simplest possible ram extrusion set up, with a cylindrical square entry die. To obtain an extrudate of length d*l,* the ram must move by a distance l_0. Assuming the paste is incompressible

$$A_0 l_0 = Al \qquad (10)$$

where A and A_0 represent the cross sectional area of the die land and barrel respectively. The work done to increase the paste length by dl with a yield stress of σ is equivalent to σAd*l*. Differentiating gives

$$\frac{dA}{A} + \frac{Adl}{A_0 l_0} = 0 \qquad (11)$$

Integrating to calculate the work done gives the equation

$$\int_{A_0}^{A} -\frac{\sigma A_0 l_0 dA}{A} = [-\sigma A_0 l_0 \ln(A)]_{A_0}^{A} = \sigma A_0 l_0 \ln\left(\frac{A_0}{A}\right) \quad (12)$$

The work done in the barrel for a pressure P_1 on the ram is given by the equation

$$W = P_1 A_0 l_0 \quad (13)$$

Equating these equations gives

$$P_1 = \sigma \ln\left(\frac{A_0}{A}\right) \quad (14)$$

where P_1 is the required pressure to force paste from the barrel into the die land, including the change in shape of the paste. It is also necessary to consider viscous effects in the liquid phase, where stress is generated relative to the strain rate. Given a liquid phase of sufficient viscosity, the stress can be written as

$$\sigma = \sigma_0 + \alpha V \quad (15)$$

where σ_0 is the yield stress of the paste, V is the velocity of the paste in the die land, and α is a constant specific to the paste which characterises the effect of velocity. Substituting equation (15) into equation (14) gives

$$P_1 = \ln\left(\frac{A_0}{A}\right)(\sigma_0 + \alpha V) \quad (16)$$

There is also a pressure drop associated with flow in the die land, P_2, where the net force is equal to $P_2\pi D^2/4$. This force is opposed by the shear at the wall, a force given by the product of the shear and the wetted perimeter, $\tau\pi DL$ for circular die lands. Equating these two fores, and rearranging for P_2 gives the equation

$$P_2 = \frac{\tau ML}{A} \quad (17)$$

where M is the perimeter. Similarly to σ in P_1, the significant viscous effects must be considered, where τ has been shown experimentally to be given by the equation

$$\tau = \tau_0 + \beta V \quad (18)$$

where τ_0 is the wall shear stress extrapolated from a velocity of zero, and β is a constant specific to the paste, characterising the effect of velocity. The total pressure drop in the die is the sum of the pressure drop required to force the paste from the barrel into the die land, and the pressure drop in the die land itself, giving a total pressure, P, of

$$P = P_1 + P_2 = \ln\left(\frac{A_0}{A}\right)(\sigma_0 + \alpha V) + \frac{ML}{A}(\tau_0 + \beta V) \quad (19)$$

In some cases, the constants α and β are not sufficient to take into account non-linear behaviour. Two parameters can be added to these terms to increase the number to six by writing the equation as

$$P = \ln\left(\frac{A_0}{A}\right)(\sigma_0 + \alpha V^m) + \frac{ML}{A}(\tau_0 + \beta V^n) \quad (20)$$

This equation is called the Benbow-Bridgwater equation, a useful tool in predicting the pressure requirement of an extrusion process.

3.2.5 Extrusion Defects and Phase Migration

During the extrusion process, there are many factors which can negatively affect the quality of the extrudate and therefore the product. In nearly all cases, it is desirable to produce an extrudate of consistent liquid content. In many cases, it may also be necessary for the extrudate to have a smooth surface. In the case of the production of BASE tubes, both of these qualities are necessary to ensure the strength of the product. Certain exit effects and phase migration during the extrusion process can give rough surfaces and sections of varying density.

Phase Migration

As mentioned previously, a paste is a highly concentrated suspension of solid particles in a shear-thinning liquid phase. When a pressure is applied to the paste, it begins to flow in the barrel and into the die land. There is a tendency for the liquid phase to move faster than the solid phase, where the ratio of speeds is dependent on the particle size distribution of the solid phase, and the rheology of the liquid phase.

In the event of significant phase migration, the initial extrudate will be rich in liquid, causing this area to have a lower density when dried. For the production of many products from a single batch of paste, this leads to inconsistency across the production which is likely to be unacceptable for most applications. Furthermore, the paste still in the barrel will have a liquid content that decreases through the process, causing a large increase in required pressure, due to the lack of excess liquid to form a lubricating layer against the barrel and die land walls. For pastes with a high solids content, the operating pressure may already be close to the upper limit of the pressure generating equipment, and any phase migration may halt the process. For large batches, this could cause significant losses of material and time.

The occurrence of phase migration is hard to anticipate in the formulation stage, but easily noticed during extrusion. A plot of ram movement against applied pressure for a constant velocity would show a positive gradient in the event of phase migration. It would normally be expected to fall over

time, as the amount of paste in contact with the barrel wall decreases, in the case of a stable paste. The extrudate will appear wet at the surface, and liquid will accumulate around the die exit in the form of droplets.

A low viscosity liquid phase favours phase migration, as it is easier for the liquid to move through the gaps between solid particles towards the die exit. The solid phase can be considered as one large porous object, with the liquid phase flowing through the pores towards the die land. For a Newtonian fluid, flowing through pores of radius R and length l, through a pressure gradient ΔP, the average liquid speed is given by the equation

$$u_m = \frac{\Delta P R^2}{8\eta l} \quad (21)$$

For a Bingham plastic, with yield stress σ and a wall shear stress τ_w, the equation becomes

$$u_m = \frac{\Delta P R^2}{8\eta l}\left[1 - \frac{4\sigma}{3\tau_w} + \frac{1}{3}\left(\frac{\sigma}{\tau_w}\right)^4\right] \quad (22)$$

The equations illustrate the relationship between viscosity and liquid phase speed, where a high viscosity liquid phase is preferable.

To reduce the effects of phase migration, in the case of the porous solid assumption, the number of "pores" can be reduced, by having a mixture of large and small particles, similar to the bimodal packing case described previously. Alternatively, more binder could be be added to give the liquid phase a high viscosity and yield stress, reducing the speed at which the liquid phase can flow.

Surface Fracture

In many applications of extruded products, it is desirable for the extrudate to have a smooth surface. This quality is particularly true in the production of BASE tubes, where a rough surface makes the formation of metal dendrites more likely during operation. Surface fractures can take the form of regular fractures following the circumference of the extrudate at regular intervals along the length, or irregular imperfections spread around the surface as shown in Figure 7 - Surface fracture in an

alumina based paste extrudate. In severe cases, the fractures can cause complete severance of the extrudate.

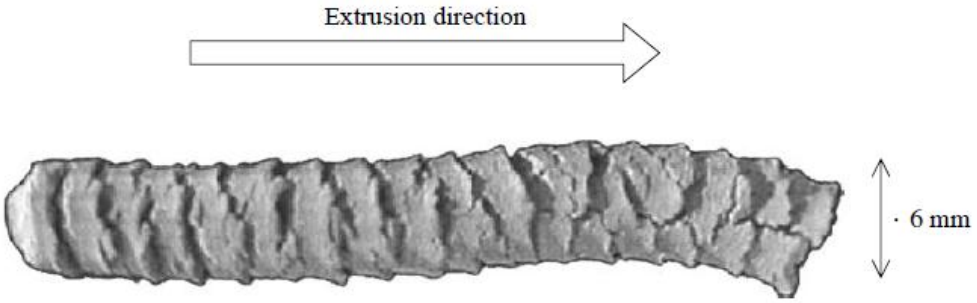

Figure 7 - Surface fracture in an alumina based paste extrudate [12]

In order for the surface to become fractured, a force parallel to the direction of flow must be present, which becomes large enough to disrupt the flow at the wall and cause a tear in the material. The tearing must then stop, as continued tearing would cause complete severance of the extrudate. This process is then repeated to provide tears all along the length of the extrudate, as shown in Figure 8.

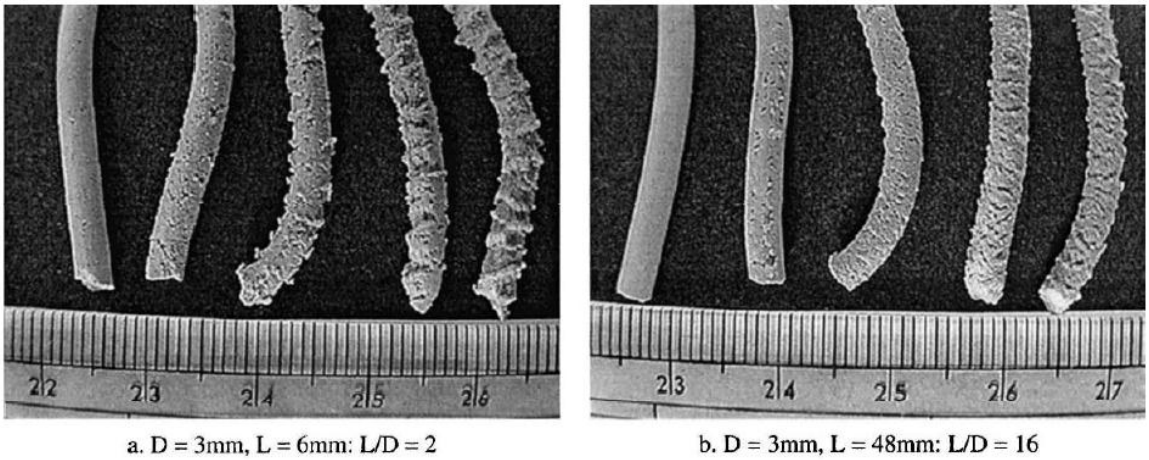

Figure 8 - Pictures of extrusion products for increasing die land velocity (increasing left to right) for L/D = 2 and 16 [13]

The effect of liquid content has also been investigated experimentally [3] [13], and it has been shown that increasing the liquid content of the paste will decrease the depth and number of fractures on the extrudate surface. Figure 9 shows the severity of surface fractures decreasing as liquid content increases.

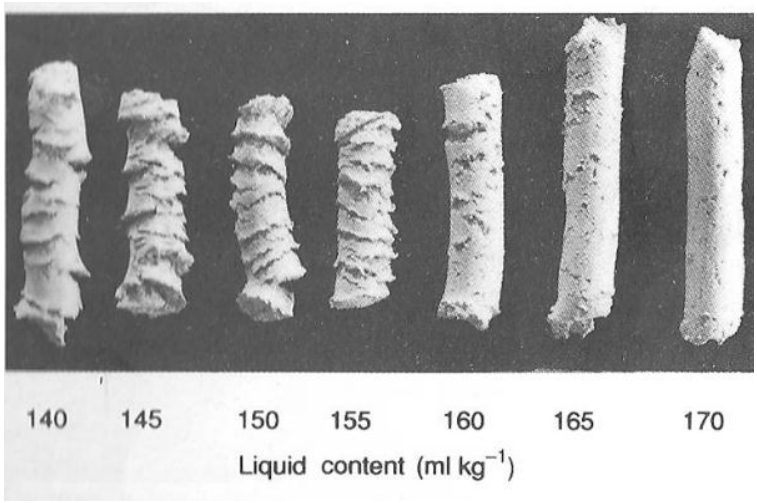

Figure 9 - Pictures of extrudates with increasing liquid content [3]

It is also possible to anticipate problems with surface fracture when designing a die for a process, with certain geometries less likely to cause defects [3].

3.2.6 Die Geometry

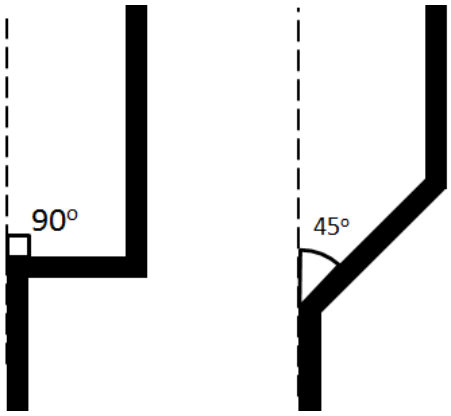

Figure 10 - Illustration of entry angle

The Benbow-Bridgwater equation is derived for the simplest extrusion geometry in the previous section – a circular, square entry die. The term square entry refers to the angle between the flow

direction and the end wall of the barrel being a right angle. Reducing the angle between these produces a tapered entry, which may be a desirable feature in the extrusion of certain products. Experiments have shown that a smaller entry angle reduces the severity of surface defects.

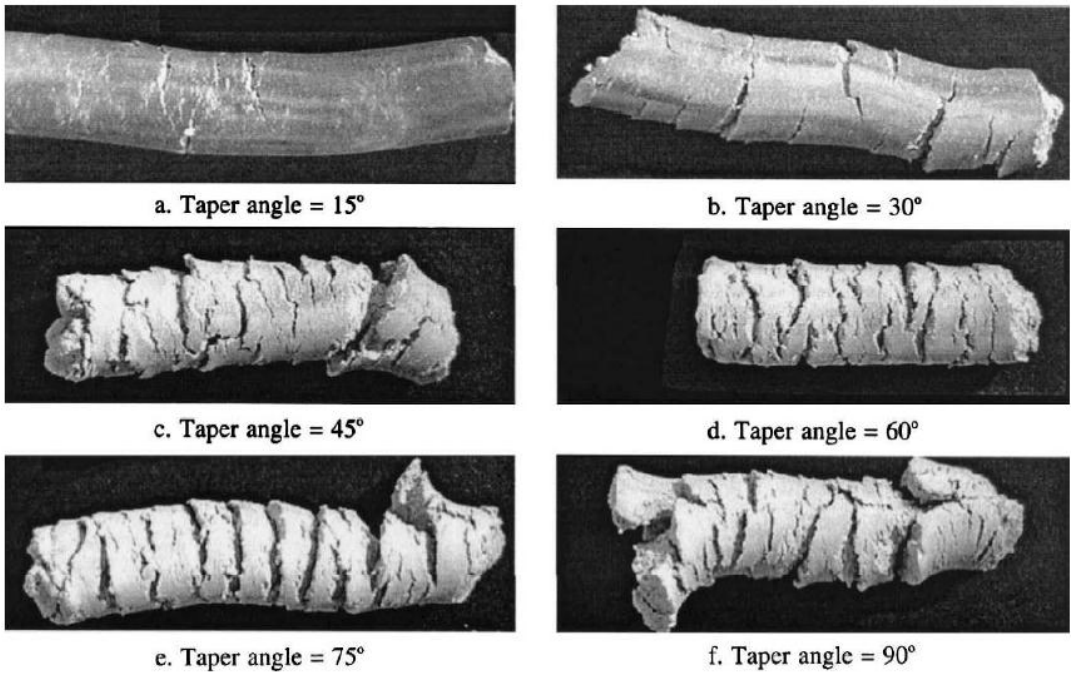

Figure 11 - Pictures to show the effect of entry angle on surface fracture severity

The use of a tapered entry forms a conical region through which the paste must flow. The tapered entry will have a larger pressure drop associated with it than the square entry die, as the paste moves across a larger surface area.

The pressure drop in the section can be calculated from the Benbow-Bridgwater equation given the terms concerning die geometry are suitably modified to take the conical entry into account.

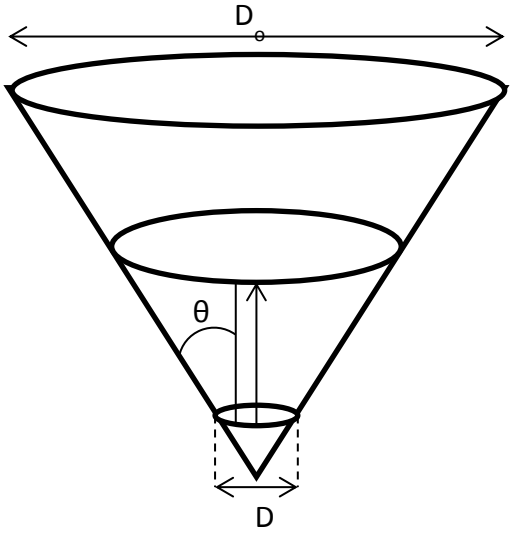

With an entry angle of θ, and a paste position of *z* from the outlet, movement through a vertical distance d*z* gives a cone

length of d*z* secθ. For wall stress τ, the resolved component of the drag force at the wall is equal to

$$\tau \cos\theta \sec\theta \, dz = \tau \, dz \qquad (23)$$

A force balance on the section dz gives

z

Figure 12 - Diagram of conical entry for predicting pressure drop

$$\frac{dp}{dz} = \frac{2\tau \cot\theta}{z} \qquad (24)$$

where p is the pressure required to overcome friction at the wall. Converting the wall stress term from the Benbow-Brigwater equation such that velocity is expressed in terms of volumetric flow rate gives

$$\tau = \tau_0 + \beta V = \tau_0 + \beta \left(\frac{Q}{\pi z^2 \tan^2 \theta} \right) \qquad (25)$$

where Q is the volumetric flow rate, which is constant regardless of paste position. Substituting equation (25) into equation (24), integrating for the whole tapered entry and then substituting into the Benbow-Bridgwater equation gives

$$P = 2\left(\sigma_0 + \frac{4\alpha Q}{\pi D^2} + \tau_0 \cot\theta \right) \ln\left(\frac{D_0}{D} \right) + \frac{4\beta Q}{\pi} \left(\frac{1}{D^2} - \frac{1}{D_0^2} \right) \qquad (26)$$

for tapered entry with a circular entrance and exit.

4. Literature Review

As the structure required to form a suitable solid electrolyte is tubular in shape, extrusion was quickly identified as a useful method in the 1970s and 80s, shortly after the initial concept had been proposed [14]. Patents filed by Ford Motor Company in 1977 [15] describe an extrusion method for "extruding a composition which may be fired to form high density β''-alumina" citing problems in the previous method, which involved pouring an aluminium oxide and sodium oxide mixture into a mould to be pressed and dried. Much of the available literature from after this time focusses on a suitable binder which can be removed before sintering, with experiments on cold extrusion binders (polyvinvyl pyrrolidone/ethylene glycol, polyvinyl alcohol), as well as hot extrusion binders (beeswax and Vaseline) [16]. Particular attention was paid to the sintering regime and post sintering characteristics, such as the β/β'' ratio.

4.1 Sodium β-Alumina Structures

Sodium β-alumina is the more well-known name of sodium hexaluminate, with the general formula $Na_{x+1}Al_{11}O_{17+(x/2)}$ where the number "x" represents the excess of sodium, balanced out by x/2 moles of oxygen due to their difference in valence (Na^+ and O^{2-}) [17], where x can be between 0 and 0.57 theoretically, although a value of around 0.3 is the most stable. It stacks hexagonally, which can be described as two spinel blocks of $Al_{11}O_{16}$, separated by a layer comprised of the remaining sodium and oxygen ions (Figure 13) [2]. These planes are referred to as "conduction planes" as they contain vacant sites which allow sodium ions to move through the structure, which gives rise to conduction in two dimensions, with a conduction value λ = 10^{-2} S cm^{-1}.

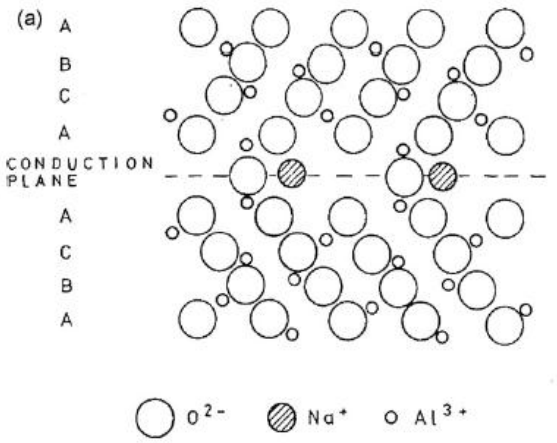

Figure 13 - Diagram of spinel blocks of sodium beta-alumina [2]

The further addition of sodium ions into the interstitial sites increases the conductivity. This can be achieved by the addition of monovalent or divalent cations, which replace the Al^{3+} ions in the spinel blocks, allowing extra sodium ions into the structure to compensate for the difference in charge. Magnesium can be added to the formulation to depart from the stoichiometric formula, allowing the formula $(Na_2O)_{1+x}$-$11Al_2O_3$ to have values of x up to 0.67 [17].

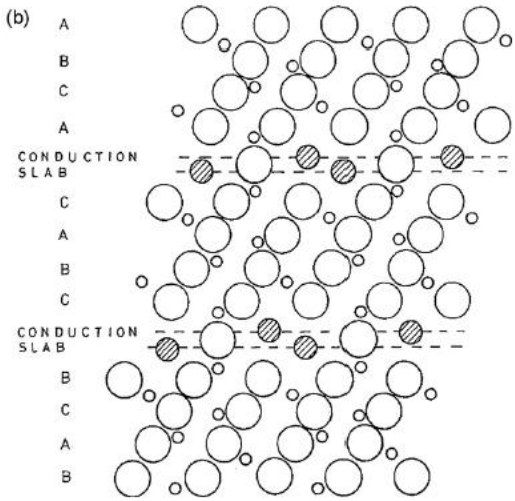

Figure 14 - Diagram to show crystal structure of β''-alumina

The use of divalent ions to stabilise β – alumina also gives rise to a different crystal structure, referred to as β''-alumina, with R_3m rhombohedral symmetry. It differs from β-alumina in that, as opposed to two spinel blocks surrounding a conductive plan, β''-alumina consists of three spinel blocks with a conductive slab separating each. This structure allows for a higher concentration of sodium ions, and therefore a higher ionic conductivity (λ = 0.2 – 0.4 S cm^{-1}) [2]. Because of this, it is this structure that is desired in the production of solid electrolytes. The production of this structure is also dependent on the conditions used in reaction-sintering of α-alumina. The highest conductivity comes from a chemical formula of $Na_{1.67}Al_{10.33}Mg_{0.67}O_{17}$ [17].

4.2 Battery Operation

The free sodium ions in sodium β-alumina make it an excellent choice for use in industrial scale batteries. The ions allow charge to be transferred between the positive and negative electrodes during charge and discharge. The ceramic's strength allows it to hold molten sodium as the cationic electrolyte, and separate it from the anionic electrolyte. In order to minimise electrical resistance, the battery is operated at around 300°C, and so the BASE must be strong and inert at this temperature to be effective. The cathode used is typically sulphur (an Na-S battery), although nickel

chloride has been shown to be effective and less corrosive to the steel case than the sodium polysulfides formed in the Na-S battery.

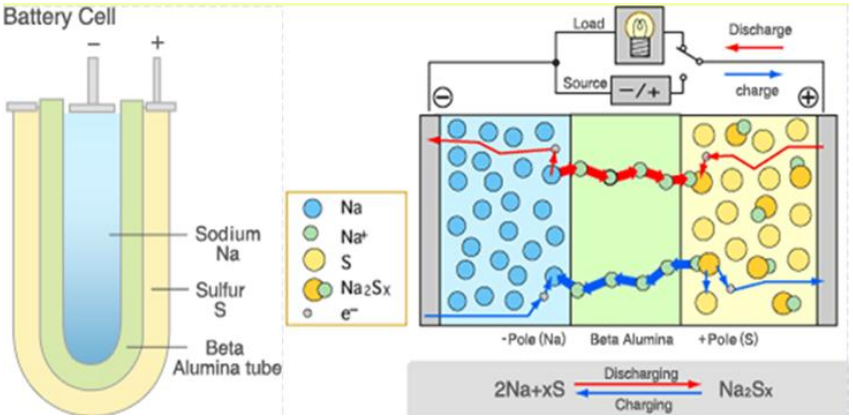

Figure 15 - Diagram of Na-S battery [19]

Figure 15 shows a diagram of the Na-S battery. During charge, sodium metal is formed inside the BASE tube, leaving sulphur on the cathode side. During discharge, sodium ions move across the electrolyte to form sodium polysulphides. The half- and overall-cell reactions are written as:

Anode: $2Na <-> 2Na^+ + 2e^-$

Cathode: $xS + 2Na^+ + 2e^- <-> Na_2S_x$

Overall: $xS + 2Na <-> Na_2S_x$ $E = 2.08V$

Due to the difficulties of handling sodium, the cell is usually assembled in the discharged state, with sodium polysulphides added. The batteries themselves are tall structures with a stainless steel case. Their small diameter means they can be put into banks for commercial use, each having an output of up to 50kW. They are more suited to non-mobile, industrial scale energy storage, although the technology was originally conceived by automobile manufacturers Ford [2].

4.3 Closed End Formation

In terms of formation of a closed end, this was done by placing a high density green ceramic disk at one end during two phase sintering, which promotes the parts attaching to each other, which produces a closed cylinder. Prior to this, a closed end was formed by pinching one end of the wet, green ceramic [14]. Merely pinching the end of the tube poses problems in modern quality control, while the method using a disc of material provides a point of weakness which could cause the battery to fail if subject to large forces during installation.

A patent filed by Ford Motor Company in 1981 [18] details a method to attach the closed end using ultrasound. A disc of sodium β''-alumina is pressed into a hemispherical shape at 150^{o}C, and then placed on the desired end of tube. The two pieces are then subjected to ultrasonic waves, which the patent says "is dissipated as heat energy which melts the thermoplastic binder composition and welds the joining surfaces".

One of the most commonly employed methods used industrially to produce BASE tubes in the UK is electrophoretic deposition. Using a negatively charged rod of the required shape in a solution of positively charged particles that make up the BASE tube causes the required material to form on the rod surface. The process is left to run until the desired thickness is achieved, at which time the rods are withdrawn and the tubes removed by sliding them off once the solid has been left to dry.

5. Experimental

5.1 Paste Formulation

The chosen method of production of BASE tubes was the extrusion of an alpha alumina paste followed by sintering and solid state reaction. In order to form the paste to be extruded, the solid powders were first mixed, with liquid added before further mixing, producing the concentrated suspension required.

The initial formulation was based on work undertaken in a previous project in the department, as well as observations made in relevant literature. The total mass of the paste was 534.62g, with the liquid added making up 13.74% of the total mass. The percentage by mass of each component is given in Table 2.

Table 2 - Initial formulation of paste

Chemical Species	Mass (g)	Mass %
α-alumina	350.56	65.6
Sodium Oxalate	79.29	14.8
Magnesium Hydroxide	16.86	3.2
Hydroxypropylmethylcellulose	6	1.1
Polyethylene Glycol	3	0.6
Yttria-stabilized Zirconia	4.07	0.8
Stearic Acid	1.5	0.3
Deionised water	73.35	13.7

Initially, each solid component was weighed out using a top pan balance, starting with the α-alumina. The α-alumina was provided by Sasol, and had a purity of 99.9% with a mean particle size of 0.8μm. α-alumina was the largest component of the paste by weight, as it is this which is

converted into β-alumina once the product is sintered. The sodium oxalate was provided by Sigma Aldrich, and was the source of the free sodium ions in the solid electrolyte giving it the ability to transfer charge. Before adding to the mixture, the sodium oxalate was ball milled for 8 hours, and then put through a Glen Creston centrifugal grinder to reduce the particle size to a mean diameter of 8 µm [20]. It was known that wet grinding leads to poor microstructure due to recrystallization. Magnesium hydroxide, reagent grade provided by Sigma Aldrich, was added to promote the formation of β''-alumina in the sintering stage. Yttria-stabilized zirconia was added to control the grain growth in the sintering stage.

The remaining components of the paste are classed as components of the liquid phase, as they are all soluble in water. Hydroxypropylmethylcellulose (HPMC) was added as a binder, to provide phase-stability in the extrusion process, as it forms a shear thinning solution in water, therefore reducing the likelihood of phase migration. The HPMC used was grade K15M, provided by Dow Chemicals, which refers to its viscosity at a certain concentration. Grade K15M means that the HPMC solution has a viscosity of 15,000 mPa.s at a concentration of 2% by mass. Polyethylene glycol (PEG) with a chain length of n=1000 was a component of the dry mixture. It is also a water soluble polymer, and provides plasticity to the paste. It is a chemical renowned for its excellent lubrication properties. Both of these polymers made the liquid phase shear thinning, theoretically allowing the paste to flow in a die under high shear, but also giving a strong, wet ceramic which can dry while retaining its shape. The stearic acid is soluble, and was also selected for its lubricating properties [21]. It also aids the interaction between the solids and the liquid polymer solution.

With both the soluble and insoluble solids weighed and measured, the powders were first mixed in a Kenwood K-blade mixer for two minutes, homogenising the dry mixture. This step was important, as on the addition of water, the binder components produce a highly viscous mixture, which would be much more difficult to homogenise. To the dry solid mixture, deionised water was added with a volume determined by previous experiments where a stable paste was observed.

In order to mix the two phases together, a Winkworth Laboratory Z-blade mixer was used. The mixer consists of a mixing container, with a large motor attached with a horizontal axle, which spins the blades. These types of mixers are common in the confectionary industry for processing extremely thick substances. The Z-blade mixer is able to provide high shear between the blades and wall. The bottom wall of the container is shaped so that it resembles two troughs with a diameter slightly larger than the width of the blade, as shown in Figure 16.

Figure 16 - Picture of Z-blade mixer used (top) and blade arrangement (bottom)

The solid mixture was removed from the Kenwood mixer and placed into the Z-blade mixer. This was left for a few minutes to spread itself around the walls and blades. The water was then added to the mixer to form a two phase mixture. The motor was set to turn at 38 rpm, with the blades rotating in opposite directions. Within a matter of seconds, it was almost always observed that most of the paste sticks to the blades, clear of the wall, where it is simply rotated with no applied shear. To prevent this, the lid was regularly opened and the paste removed from the blades using a knife. The frequency of this action decreased as the mixing process went on as the cohesion between the solid particles became greater, and the middle peak in the bottom surface (Figure 16) was able to remove paste from the blade without external interference.

The end point of mixing was a subjective one in the absence of a torque meter, which would indicate a steady value once the mixture was homogenous. Instead, the paste was judged based on its appearance. Indications of the paste being well mixed were a consistent colour and texture, and no areas where the moisture content is obviously higher, indicated by a shiny surface. Once the end

point was reached, the side wall was removed and the paste taken out and placed in a polythene bag. This bag was placed in a refrigerator, to reduce the vapour pressure of water, retaining the water in the paste rather than the air in the bag.

5.2 Small Scale Extrusion

In order for the strengths and weaknesses of the paste to be assessed, it was first necessary to test it through extrusion on a small scale. Performing these tests allowed the Benbow Bridgwater parameters to be obtained, which allowed the paste to be characterised. Changes could then be made to the formulation, and further tests carried out to obtain data for plots of yield stress against moisture content.

Once the paste had been left for 24 hours in the refrigerator, it was removed and loaded into a small barrel, with a diameter of 25.4 mm. The barrel had three different interchangeable die lands to be fitted at the end, with different L/D ratios. The diameter of each was 3mm, and the L/D values were 1, 8 and 16. Paste was loaded into the die in small pieces, and a mallet and metal rod were used to pack the paste into the barrel ensuring as few air bubbles as possible were present. This process was repeated until the barrel was filled to 10mm from the top, at which point the ram was inserted.

To carry out ram extrusion, the downwards pressure was generated by an Instron 4467 load frame, which was mounted on a bench. The load frame was fitted with a load cell, with a capacity of 30 kN. The Instron generates pressure using lead screws, which move the crosshead by a distance measured by the number of screw rotations, shown in Figure 17. The Instron is

Figure 17 - Instron load frame in laboratory

capable of many functions, including strength testing. However for this application, the machine was programmed to move downwards at a series of speeds. The paste was extruded at ram velocities of 1, 2, 5, 10, 20 and 50 mm/min, for all 3 values of L/D. At each speed, the extrusion was allowed to continue for a set ram displacement of 5 mm.

For each speed, the average pressure was taken and the data plotted as a graph of pressure against L/D, and pressure against velocity. The plot of pressure against velocity allowed the Benbow-Bridgwater parameters of the paste to be calculated through curve fitting (see Figure 18). The attached computer had software which performed the calculations to obtain all 6 parameters in equation 26 [22].

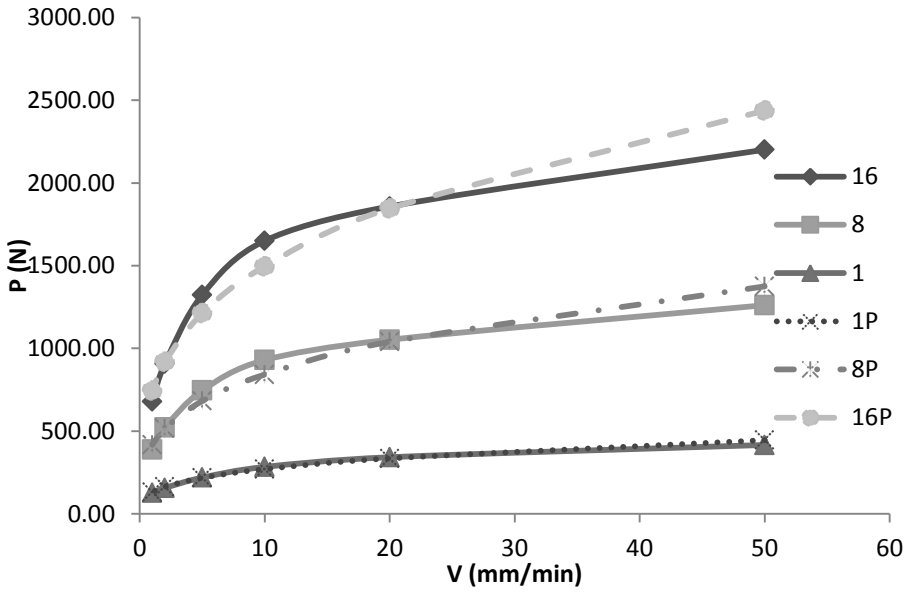

Figure 18 - Experimental data (solid lines) with Benbow-Bridgwater models (dashed lines)

Figure 18 shows the experimental data fits the Benbow-Bridgwater equation best at low speeds and low values of L/D, with the lines diverging above ram velocities of 20 mm/min. This is far below what would be used in the production of BASE tubes.

5.3 BASE Tube Extrusion

The BASE tubes were extruded in a similar way to the small scale extrusion experiments; albeit with more paste and a more complex die. The differences lie in the production of a closed end, which involves manual intervention during the process. In order to produce a hollow tube with a domed, closed end, the die geometry was significantly more complicated than those used in paste characterisation.

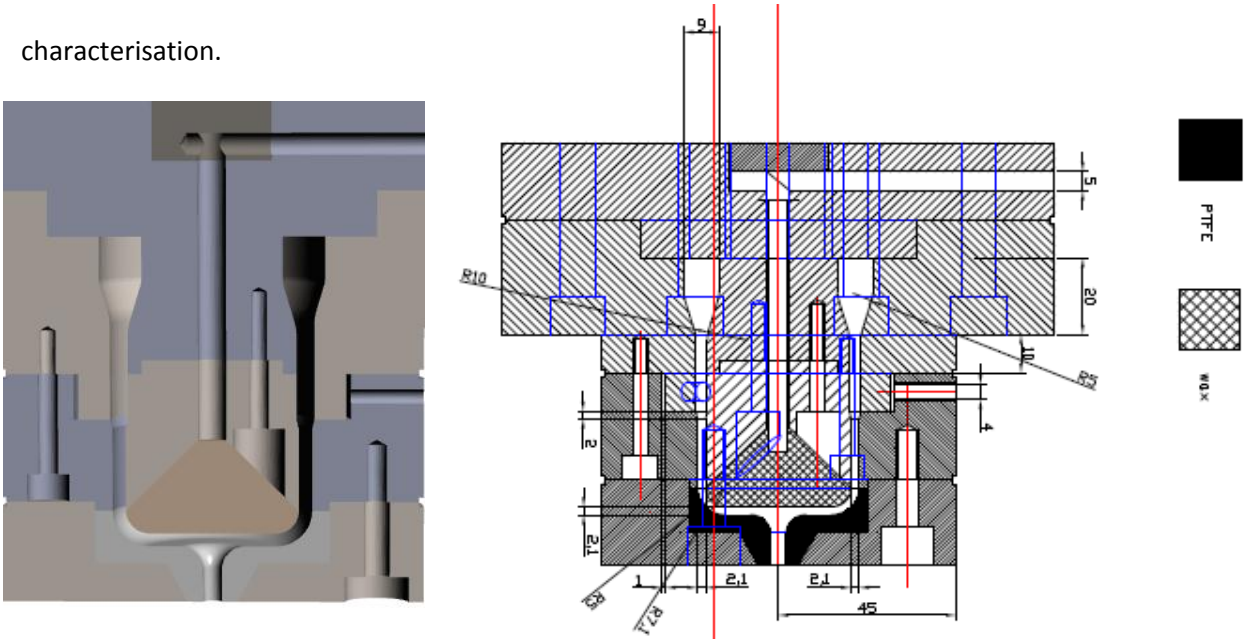

Figure 19 - Technical drawings of die used in its manufacture

Figure 19 shows the technical drawing from which the die was manufactured, showing some of the materials and dimensions of the die. The diagram on the right shows the materials PTFE and wax, both of which form part of the closed end cap. The die could be used without this cap, which consists of everything shown in Figure 19 below the wax insert, producing hollow tubes of material. It is between the wax and PTFE that the paste which forms the closed end flows through, with these materials chosen for their low adhesive properties. After formation, the cap was removed, and extrusion continued, once the wax had been dislodged from the conical end of the central pin.

The die can be broken down into 9 stages, starting at the barrel exit, and ending at the small outlet in the closed end cap, shown in Figure 20 . The paste flowed from the barrel into a series of channels of decreasing cross-sectional area. The majority of the die length resembles annular flow, where the

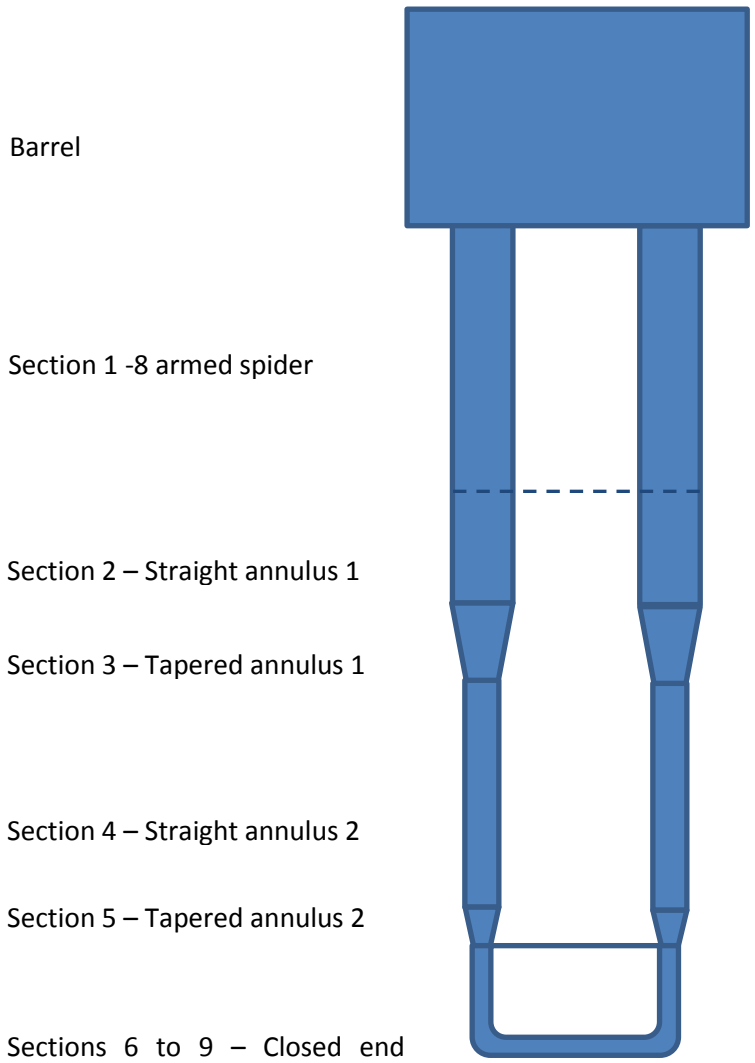

Figure 20 - Diagram of flow arrangement inside die (not to scale)

paste flows around the central pin. This feature is essential to the formation of a hollow tube.

The die consisted of several pieces which screwed together. This was necessary to produce such a complex arrangement, and also had advantages when cleaning. Attached to the barrel was a large piece containing section 1 and the central pin. This also contained the wax seal-breaking mechanism, with the force applied via a perpendicular rods, one of which goes through one of the arms of the spider. After this point, two rings of steel were attached, with the inside of each complementing the surface of the centre pin to form the flow arrangement shown in Figure 20. It is after this piece where the majority of the BASE tube will exit, and it was therefore important to ensure the central pin and the walls of this piece were aligned correctly. To prevent this piece from tilting in relation to the previous parts there is a small section of overlap between the pieces, where three screws are equally positioned around the circumference, which were used to correct any misalignment after assembly.

Figure 21 - Fully assembled die and ram

At this point the wax was attached to a conical insert on the end of the central pin; initially, the seal is closed, and the paste flows around the wax to form the closed end. Once the shape has been formed, the seal is broken by applying force through the centre pin, which forces the seal to break, allowing air to flow inside for extrusion of the tube to continue without the tube collapsing in on itself. The force is applied through two perpendicular steel rods, as shown at the expense of the spider in Figure 19. The wax piece was first attached using an adhesive, and then a soldering iron was used to form a seal around the edge, preventing the paste from flowing underneath. The final piece was the closed end cap, which had a PTFE insert to complement the wax surface, allowing paste to fill the space between the two with the desired thickness.

Once the die had been assembled, and the wax seal attached, the paste was loaded into the barrel of the die in much the same way as the small scale experiments. In this case, the barrel was much larger, making it much more difficult to remove the air bubbles. The die was then placed on a stand on the load cell. For this extrusion, a different Instron was used with a capacity of 100 kN, where the piston was stationary at the top, and die moves upwards towards it on a central platform. The platform speed was set to 6mm/min, and the extrusion left to run until paste was seen emerging from the bottom of the die. At this point, the Instron was stopped and the end cap of the die removed. If the extrusion was successful up to this point, this should reveal the PTFE insert in the cap, or the paste shaped into a closed end. Using a hammer, force was applied to the wax breaking mechanism, and the extrusion continued until the barrel was empty. Small screws in the side of the die exit allowed the centre pin and surrounding pieces to be aligned during operation if it was observed that a misalignment was preventing the production of a straight extrudate.

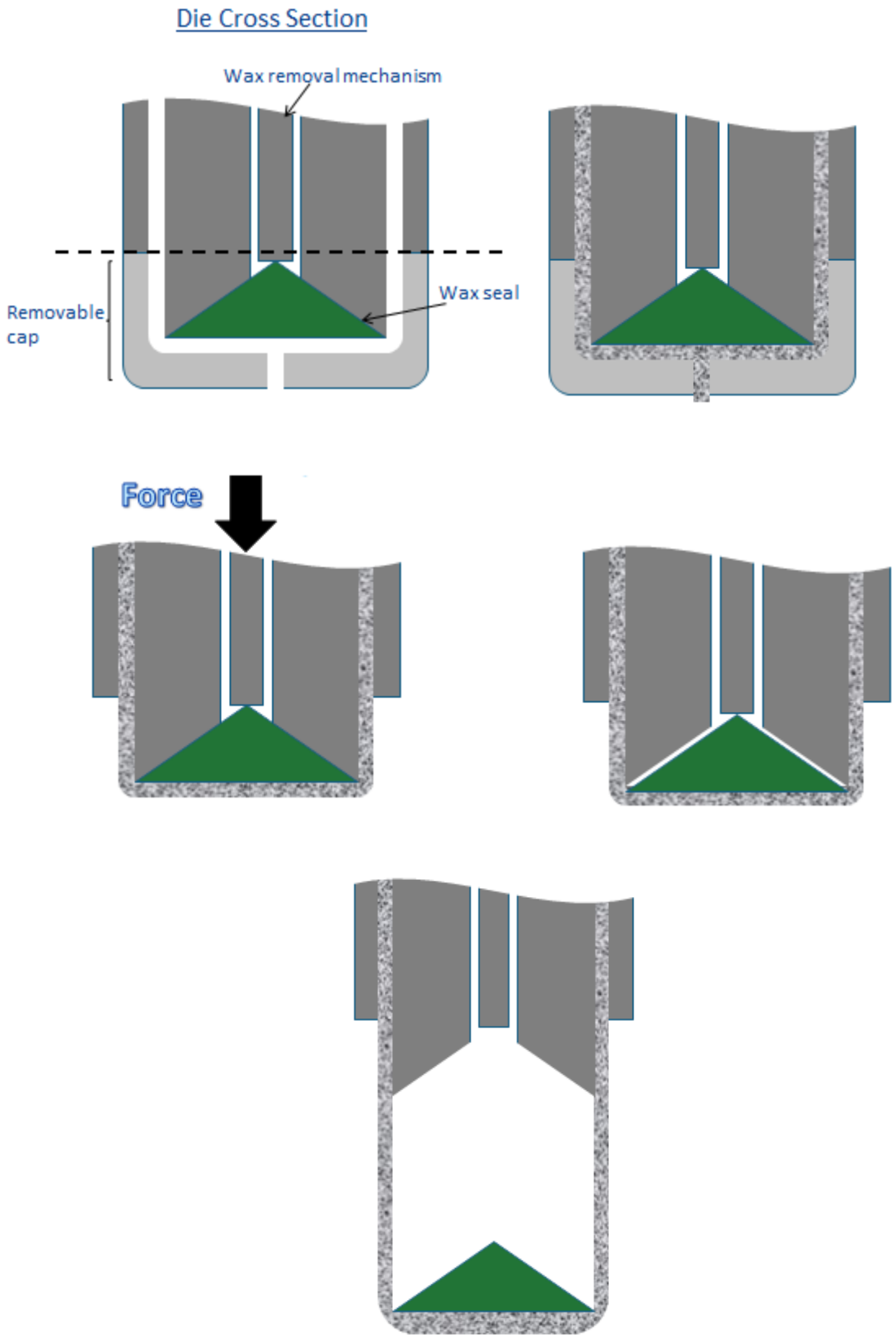

Figure 22 - Set of diagrams to illustrate closed end mechanism, from top left to bottom centre, showing the die filling, the removal of the cap, the applied force and opening of air channels to allow extrusion to continue

6. Extrusion Modelling

Producing a product through extrusion requires a pressure dependent on the rheology of the paste. In some cases, the pressure required to extrude a paste may be extremely high, governing the price of apparatus which must be designed to comfortably take such loads. In industrial processes, the die and supporting equipment will be subject to these forces regularly over a period of years. It may be useful in the design process therefore, if the maximum pressure that the apparatus will eventually be required to withstand is known.

Predictions of this nature would also be useful in the case of a process changing the formulation of a paste. A change in paste rheology may cause the extrusion pressure to increase beyond the safe limits of the apparatus, and so the process is inherently safe through the use of small scale extrusions, followed by analysis and predictive modelling.

The modelling of the die used to extrude closed end BASE was performed using the Benbow Bridgwater equation, which relates pressure to velocity as follows;

$$P = \ln\left(\frac{A_0}{A}\right)(\sigma + \alpha V^m) + \frac{ML}{A}\,(\tau + \beta V^n) \qquad (27)$$

where the variables are as described in section 3.2.4 Paste Extrusion. This equation can be modified to apply to almost any die geometry, which makes it particularly useful for this application, where the die has a complex structure consisting mainly of flow through an annulus. The equation is also chosen for its simplicity, with only 2 terms and no time dependency. The parameters m and n are often assumed to be 1 in the so-called 4 parameter model, which allows many pressure drop predictions to be made quickly and easily.

Another possible method is the Herschel-Bulkley equation, which relates shear stress to yield stress and shear rate;

$$\tau = \tau_0 + K\dot{\gamma}^n \quad (28)$$

However this equation is difficult to apply to the geometries employed in the die, i.e. flow through an annulus, concentric flow, tapered annulus, as the Navier-Stokes equation simplifies using boundary conditions for speed at the walls and the centre of the pipe.

6.1 Die Geometry

The Benbow-Bridgwater equation is commonly used to great effect in predicting the pressure drop in a square entry die with a cylindrical barrel and die land. This allows the equation to be simplified into a function of the diameter (D) of each section, rather than the area (A) and perimeter (M). Substituting the formula for the area and perimeter of a circle into equation

$$P = \ln\left(\frac{A_0}{A}\right)(\sigma + \alpha V^m) + \frac{ML}{A}(\tau + \beta V^n) \quad (27)$$

$$P = \ln\left(\frac{\pi D_0^2}{\pi D^2}\right)(\sigma + \alpha V^m) + \frac{\pi DL}{\frac{\pi D^2}{4}}(\tau + \beta V^n) \quad (29)$$

Cancelling out π and D terms gives

$$P = 2\ln\left(\frac{D_0}{D}\right)(\sigma + \alpha V^m) + \frac{4L}{D}(\tau + \beta V^n) \quad (30)$$

Similarly, it will be sometimes useful to substitute in equations for the area or perimeter of other die land and barrel shapes, and allow simplifications to be made.

6.1.1 Assumptions

As the Benbow-Bridgwater model is a simple technique for predicting the pressure drop through a die, assumptions must be made to use it suitably for a die of this complexity.

1. Paste is incompressible – this allows the velocity of the paste in the die land to be calculated from the ram velocity and the ratio of barrel area to die land area

2. Paste is perfectly packed into barrel – this assumption relates to air pockets in the barrel when the paste is loaded, where pushing the air pockets out requires displacement of the ram with no paste movement
3. Plug flow – the velocity and distance travelled along the die do not vary across a cross-section

6.1.2 Section 1 – Spider

Immediately after the barrel, the paste enters 8 equally sized holes, with "arms" dividing the space between them, collectively called a spider. This arrangement allows the flow to enter the hollow cylindrical arrangement eventually required, but it also serves a purpose regarding the closed end formation. One of the spider's arms is hollow and contains one piece of the wax removal mechanism, shown in the top of the diagrams in Figure 19.

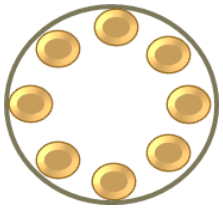

The section features 8 cylindrical channels, each with a diameter of 9mm, and a length of 30 mm. The pressure drop for this section can be calculated from equation (27), by substituting in the total area of all 8 holes. The same principle was used for the perimeter, giving the equation

$$P = \ln\left(\frac{A_{barrel}}{\mathrm{n}A_{holes}}\right)(\sigma + \alpha V^m) + \frac{\mathrm{n}M_{holes}L}{\mathrm{n}A_{holes}}(\tau + \beta V^n) \quad (31)$$

$$P_1 = \ln\left(\frac{A_{barrel}}{8A_{holes}}\right)(\sigma + \alpha V^m) + \frac{M_{holes}L}{A_{holes}}(\tau + \beta V^n) \quad (32)$$

where the subscript "holes" refers to the area or perimeter of an individual hole, and n is the number of holes, in this case 8.

6.1.3 Section 2 – Straight annulus 1

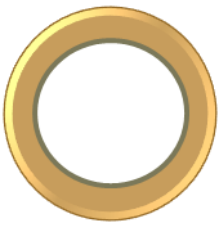

After exiting the spider, the paste enters an annulus, where the total area is equal to the area of the holes and arms in the previous section. As such the cross sectional area of the flow increases between this section and the previous one.

In order to calculate the cross sectional area of an annulus, the difference between the areas of the circles formed by the outer and inner diameters of the section was calculated. Let A_1 denote the flow area of the previous section, A_i and D_i denote inner diameter, and A_o and D_o denote outer diameter, giving the Benbow-Bridgwater equation as;

$$M = \pi(D_o + D_i) \tag{33}$$

$$P = \ln\left(\frac{A_1}{A_o - A_i}\right)(\sigma + \alpha V^m) + \frac{\pi(D_o + D_i)L}{A_o - A_i}\,(\tau + \beta V^n) \tag{34}$$

$$A_o - A_i = \frac{\pi D_o^2}{4} - \frac{\pi D_i^2}{4} = \frac{\pi}{4}(D_o^2 - D_i^2) \tag{35}$$

Substituting (35) into (34) gives

$$P_2 = \ln\left(\frac{4A_1}{\pi(D_o^2 - D_i^2)}\right)(\sigma + \alpha V^m) + \frac{4(D_o + D_i)L}{(D_o^2 - D_i^2)}\,(\tau + \beta V^n) \tag{36}$$

This, however, gives a negative overall pressure drop due to the increase in cross sectional area, making the first term of equation 36 negative, and larger in magnitude than the second term. The second term itself is not valid in this case, as the paste does not expand to fill the section and touch the whole perimeter. Instead, the paste comes out as 8 tubes of material, with no additional pressure increase until the section is full, at which point the pressure begins to increase until flow can continue into the next section. As such, the pressure drop for this section was assumed to be zero.

6.1.4 Section 3 –Tapered Annulus 1

The next section of the die is a tapered annulus, where the flow area decreases along the direction of flow. Benbow and Bridgwater devised a method of calculating pressure drop through a tapered section of a die analytically (see 3.2.4 Paste Flow), while other numerical methods [23] have been shown to give accurate predictions. However, the existing methods focus on tapered circular ducts, rather than annular flow. For this reason, a numerical method was applied to evaluate the pressure drop through the tapered annulus.

The tapered section was split into a number of “steps” where the pressure drop is calculated between each step and the sum taken.

Figure 23 - Diagram of "steps" used to calculate pressure drop in tapered annulus

In this section it was assumed that the outer and inner diameter of the annulus change at the same rate, although the inner diameter changes by 5.9 mm, while the outer diameter decrease by 4.6 mm. Assuming both change by 5.25 mm allowed simplifications to be made in the calculation of the flow area.

Given N iterations for a total section of length L, the die land length (H), inner and outer diameters ($D_{i,n}$ and $D_{o,n}$) can be calculated for each step. Assuming outer and inner diameters change by the same amount in each step, x;

$$H = \frac{L}{N} \quad (37)$$

$$\left(\frac{D_{i,exit} - D_{i,entry}}{N}\right) = \left(\frac{D_{o,entry} - D_{o,exit}}{N}\right) = x \quad (38)$$

$$D_{o,n} = D_{o,entry} - nx \quad (39)$$

$$D_{i,n} = D_{i,entry} + nx \quad (40)$$

where the subscript n denotes the iteration number. The area at any point was then calculated using the equation

$$A_n = \pi\left(\left(\frac{D_{o,n=0} - nx}{2}\right)^2 - \left(\frac{D_{i,n=0} + nx}{2}\right)^2\right) \quad (41)$$

$$= \frac{\pi}{4}\left(D_{o,n=0}^2 - D_{i,n=0}^2 - 2nx\left(D_{o,n=0} + D_{i,n=0}\right)\right)$$

where the subscript n=0 is used to indicate the variable at the entrance to the tapered section. A similar calculation was performed to find the perimeter at any point, by substituting (39) and (40) into (33)

$$M_n = \pi\left(D_{i,n=0} + nx + D_{o,n=0} - nx\right) = \pi\left(D_{i,n=0} + D_{o,n=0}\right) = \text{ constant} \quad (42)$$

This result is significant, as it shows that the die land perimeter does not vary along the length of the section. This was substituted into equation (41) to give

$$A_n = \frac{\pi}{4}\left(D_{o,n=0}^2 - D_{i,n=0}^2\right) - \frac{Mnx}{2} = A_{n=0} - \frac{Mnx}{2} \quad (43)$$

where $A_{n=0}$ is the area at the entrance to the section. Equation (43) allowed the velocity to be calculated at any point. The total pressure drop through the section, was therefore given by the equation

$$P_3 = \sum_{n=0}^{n=N} \ln\left(\frac{A_{n-1}}{A_n}\right)(\sigma_0 + \alpha V) + \frac{MH}{A_n}(\tau_0 + \beta V) \quad (44)$$

6.1.5 Section 4 – Straight Annulus 2

In this section, the paste enters at exactly the same flow area and geometry as when it leaves. The first term of the Benbow-Bridgwater equation therefore reduces to zero in the absence of any shape, leaving all increase in ram pressure to be caused by shear stress at the wall.

$$P_4 = \frac{ML}{A}(\tau_0 + \beta V) \quad (45)$$

6.1.6 Section 5 – Tapered Annulus 2

In this section, the method used to calculate the pressure drop is much the same as in the previous tapered annulus. It was still assumed that the inner and outer diameter changed by the same amount, an assumption which was more valid than in the first tapered section, with changes of 1.1mm and 0.9mm in the inner and outer diameters respectively.

$$P_5 = \sum_{n=0}^{n=N} \ln\left(\frac{A_{n-1}}{A_n}\right)(\sigma_0 + \alpha V) + \frac{MH}{A_n}(\tau_0 + \beta V) \quad (46)$$

6.1.7 Section 6 – Closed end

The flow arrangement to create a closed end consists of a straight annulus which begins to converge through a 90 degree angle, after which the paste flows in the horizontal direction only towards the central axis of the die. After this point, the paste flows downwards through a small outlet, used to indicate the formation of the closed end to the operator.

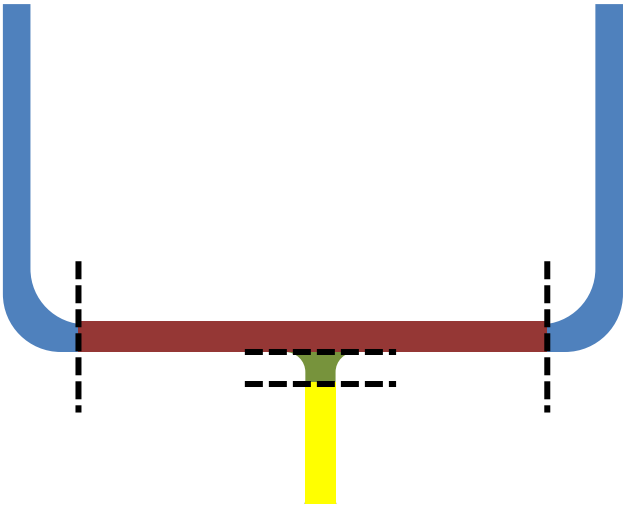

Figure 24 - Diagram of closed end arrangement and subsections used for modelling (not to scale)

Section 6.1 – Straight Annulus 3

The first section of the closed end was taken to be a straight annulus up until the point where the flow has turned a full 90 degrees, with the assumption that in the process of turning, the pressure required is no different to that when moving in a straight line. Indeed, the wall thickness of the closed end is constant everywhere, and so the difference in area for this corner is assumed to be negligible. As the flow area is constant for the whole section, again the first term of the Benbow-Bridgwater equation reduces to zero in the absence of a shape change, and so all additional ram pressure required is solely down to wall stress.

$$P_6 = \frac{ML}{A}(\tau_0 + \beta V) \qquad (47)$$

Section 6.2 – Converging Radial Flow

In this section, the paste converges from the outside of the die towards the central hole, resulting in a disc of material which forms the closed end. The geometry involved in modelling this section was different to all previous sections; however it was still possible to use the Benbow-Bridgwater equation.

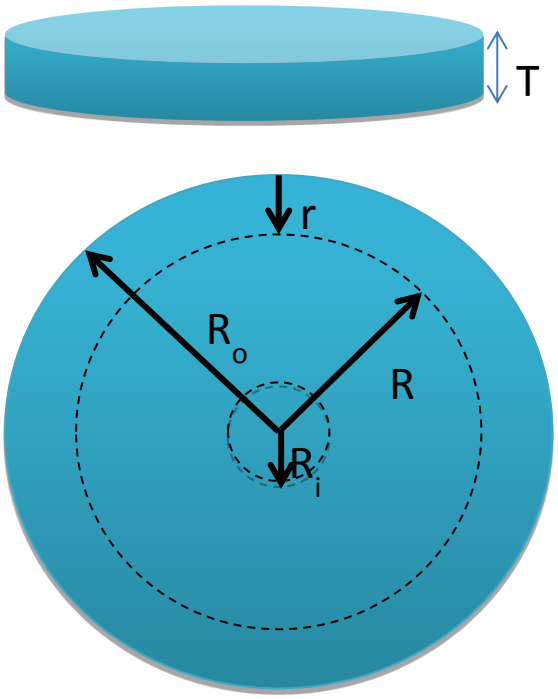

The radius of the disc was taken to be R_0, the radial position at which all the paste enters the section. At the centre of the disc, the paste flows out downwards, a position which was termed R_i. As the paste moves into the disc, its radial displacement from the entrance was termed r, and its radial distance from the edge of the outlet hole termed R, where

$$R = R_o - r \quad (48)$$

This disc has a constant thickness T, which allowed the total cross sectional flow area at any point to be calculated by the equation

$$A = 2\pi RT \quad (49)$$

Similarly for the perimeter

$$M = 4\pi R \quad (50)$$

Substituting equation (50) into equation (49) gives

$$A = \frac{MT}{2} \quad (51)$$

By dividing the disc into many increments of r, and calculating the pressure drop through the Benbow-Bridgwater equation, the overall pressure drop required to move the paste from the edge of the disc to the centre hole was calculated.

$$P_7 = \sum_{n=0}^{n=N} \ln\left(\frac{A_{n-1}}{A_n}\right)(\sigma_0 + \alpha V) + \frac{MH}{A_n}(\tau_0 + \beta V) \quad (52)$$

Section 6.3 "Trumpet"-shaped section

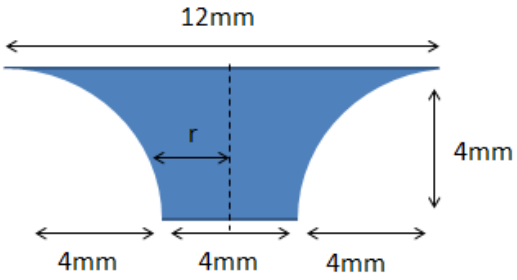

Figure 25 – Vertical cross-section of "trumpet"-shaped section of closed end forming section of die

Figure 25 shows the next section of the die, a "trumpet"-shaped section, akin to a tapered section where the diameter decreases less rapidly along the direction of flow. In order to solve the pressure drop through an arrangement like this, the relationship between distance along direction of flow, z, and diameter first had to be quantified, and a general equation found.

As the change in radius and length of the section were found to be the same, when taking a vertical cross section, the area either side of the flow were considered to be two quarter-circles, each with a radius, R, of 4 mm.

Figure 26 shows how this was used to calculate r at any point. A triangle was constructed using the radius, R, such that the hypotenuse joins the centre of the quarter-circle with the point at which the flow area is to be calculated. The other two sides of the triangle were the difference between the total length of the section and the distance travelled by the paste into the section (L-z), and the difference between the entry radius and the radius at the point at which the flow area is to be calculated (x).

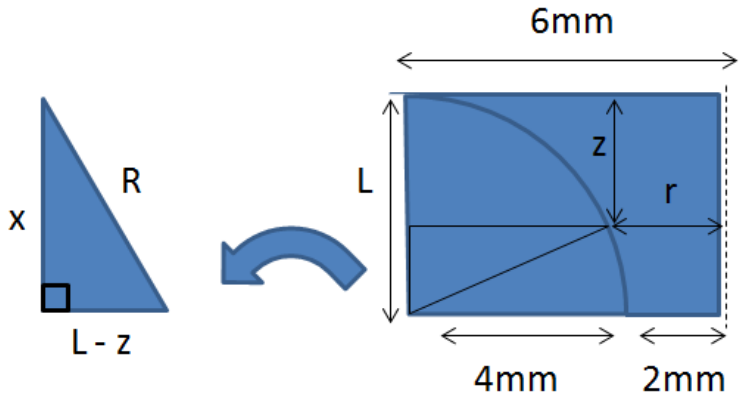

Figure 26 - Diagram illustrating method used to calculate flow area

From this triangle, x can be calculated using the Pythagoras theorem

$$R^2 = x^2 + (L - z)^2 \quad (53)$$

$$x^2 = R^2 - (L - z)^2 \quad (54)$$

Equation (54) resembles that of a Cartesian circle, where "L – z" represents the y-axis value of a circle plotted about the origin on a graph. The section was split into discrete steps where the pressure drop was calculated for each. For N steps of height H, this gave the general equations for the area and perimeter as

$$A = \pi\left(r_0 - \sqrt{R^2 - (L - nH)^2}\right)^2 \quad (55)$$

$$M = 2\pi\left(r_0 - \sqrt{R^2 - (L - nH)^2}\right) \quad (56)$$

The total pressure was given by the equation

$$P_8 = \sum_{n=0}^{n=N} \ln\left(\frac{A_{n-1}}{A_n}\right)(\sigma_0 + \alpha V) + \frac{MH}{A_n}(\tau_0 + \beta V) \quad (57)$$

Section 6.4 – Straight tube

The final section of the closed die is a simple tubular section, where the cross sectional area remains constant from the exit of the previous section, giving the equation.

$$P_8 = \frac{ML}{A}(\tau_0 + \beta V) \quad (58)$$

7. Results and Discussion

7.1 Solid to Binder Ratio

The material properties for the starting formulation were obtained using small scale extrusion, with varying velocity and L/D (ratio of die land length to extrudate diameter) independently.

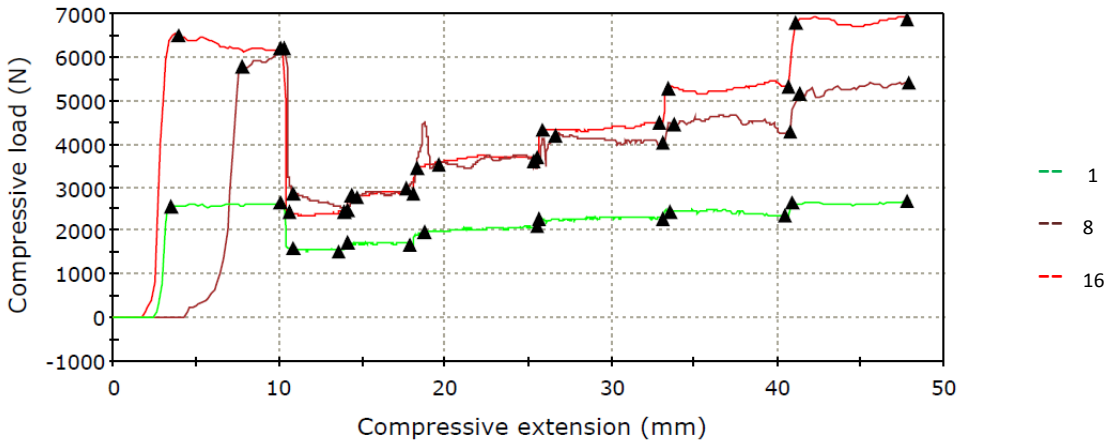

Figure 27 - Graph to show extrusion pressure against compressive extension for L/D = 16, 8 and 1

Figure 27 shows the results of a small scale extrusion using the original formulation. The "steps" visible indicate the different ram velocities; 50, 1, 2, 5, 10, 20 and 50 mm/min from left to right. In this figure, it can be seen that the pressure sometimes undergoes large, temporary increases or decreases. The black triangles indicate the portions over which an average pressure was taken for each velocity, in an attempt to gain more accurate results for use in the calculation of the material properties. The fluctuations arise from air bubbles in the barrel, which are more difficult to remove with a stiffer paste. As a result, measuring the material properties for this paste was difficult to do accurately.

Following this result, the solid to binder ratio was decreased in increments of 1% of the solid mass, with the original formulation comprising 16.2% binder.

Table 3 - List of formulations of alpha-alumina paste

Liquid Phase Content	16.2		17.2		18.2	
	mass (g)	%	mass (g)	%	mass (g)	%
α-Alumina	300	65.54%	295.4	64.5%	292.8	63.97%
Na Ox.	67.9	14.83%	66.9	14.6%	66.3	14.48%
MgOH	14.4	3.15%	14.2	3.1%	14.1	3.07%
HPMC	5.1	1.12%	5.5	1.2%	5.8	1.26%
PEG	2.6	0.56%	2.7	0.6%	2.9	0.63%
Zr	3.5	0.76%	3.7	0.8%	3.9	0.86%
DI H2O	62.9	13.74%	66.8	14.6%	70.7	15.44%
Stearic	1.3	0.28%	1.3	0.3%	1.3	0.28%

The two new pastes were tested in exactly the same way as the original formulation, with the material properties calculated from the relationship between pressure, velocity and L/D ratio. Obtaining an average pressure for each velocity at each value of L/D allows two graphs to be produced; pressure against velocity, and pressure against L/D with the amount of series of data being equal to the number of L/D or velocity values respectively.

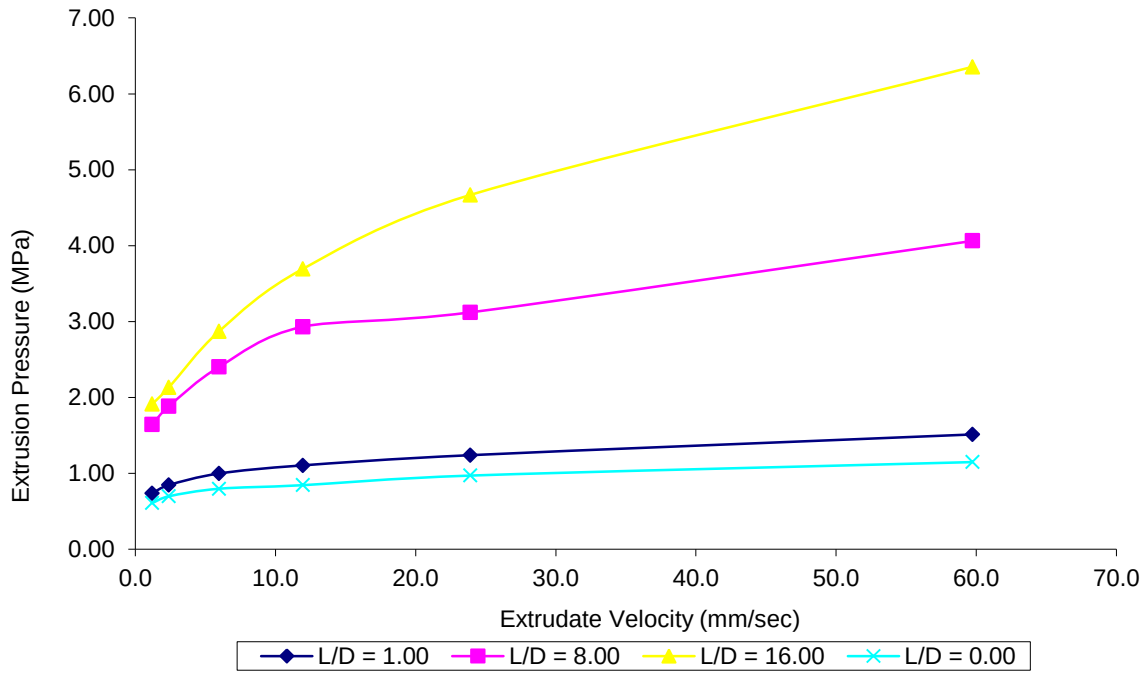

Figure 28 - Graph to show extrusion pressure against extrudate velocity for a paste of 18.2% binder

Figure 28 shows a graph of pressure against velocity for the softest paste. Included is a set of values for L/D = 0, which is obtained from a separate graph of pressure against L/D, by reading the y-intercepts of each series. From pressure values obtained by setting V and L/D to zero, the Benbow-Bridgwater equation can be manipulated to obtain the material properties. For simplicity at this stage, only the four parameter Benbow-Bridgwater equation was used, i.e. the linear form, with powers "m" and "n" set to 1.

Table 4 - Benbow-Bridgwater Parameters for the tested pastes

4 Parameter Results					
Property	16.2%	16.2%	17.2%	18.2%	16.7%
σ (MPa)	3.231	0.636	0.378	0.140	0.411
α (MPa.s.m^{-1})	32.35	7.039	0.954	2.159	3.524
τ (MPa)	0.068	0.077	0.045	0.031	0.0411
β (MPa.s.m^{-1})	5.478	1.808	1.931	1.003	1.217

Collecting extrusion data gave a good idea of a paste's suitability, but it was also necessary to carefully examine the extrudate while bearing in mind the end application. As the aim was to produce a long tube which hangs from the die, the paste with 18.2% binder was deemed unsuitable, as it would most likely detach from the die under its own weight. The paste with 17.2% binder was observed to stick to metallic surfaces, making it impractical from an experimental point of view.

The most concentrated paste was tested twice, and a large difference was observed between the two pastes. This could be attributed to the small amount of water in the formulation, causing any evaporation during mixing to have a profound effect on the paste's behaviour. This paste is close to the maximum packing fraction for bimodal systems [24], and as such any further decrease in the liquid phase volume due to evaporation has a disproportionately higher effect on the yield stress. This result also illustrates the difficulties in producing pastes with consistent properties between batches, particularly at this level of solids concentration.

As the 16.2% binder paste was extremely stiff, and the 17.2% binder paste too adhesive owing to excess water, this was established as the window of operation, and a paste was produced between these two values, which is shown in Table 3 as 16.7% binder. This paste produced a smooth extrudate, which dried quickly to produce a hard solid, and was seen as the best paste for further evaluation.

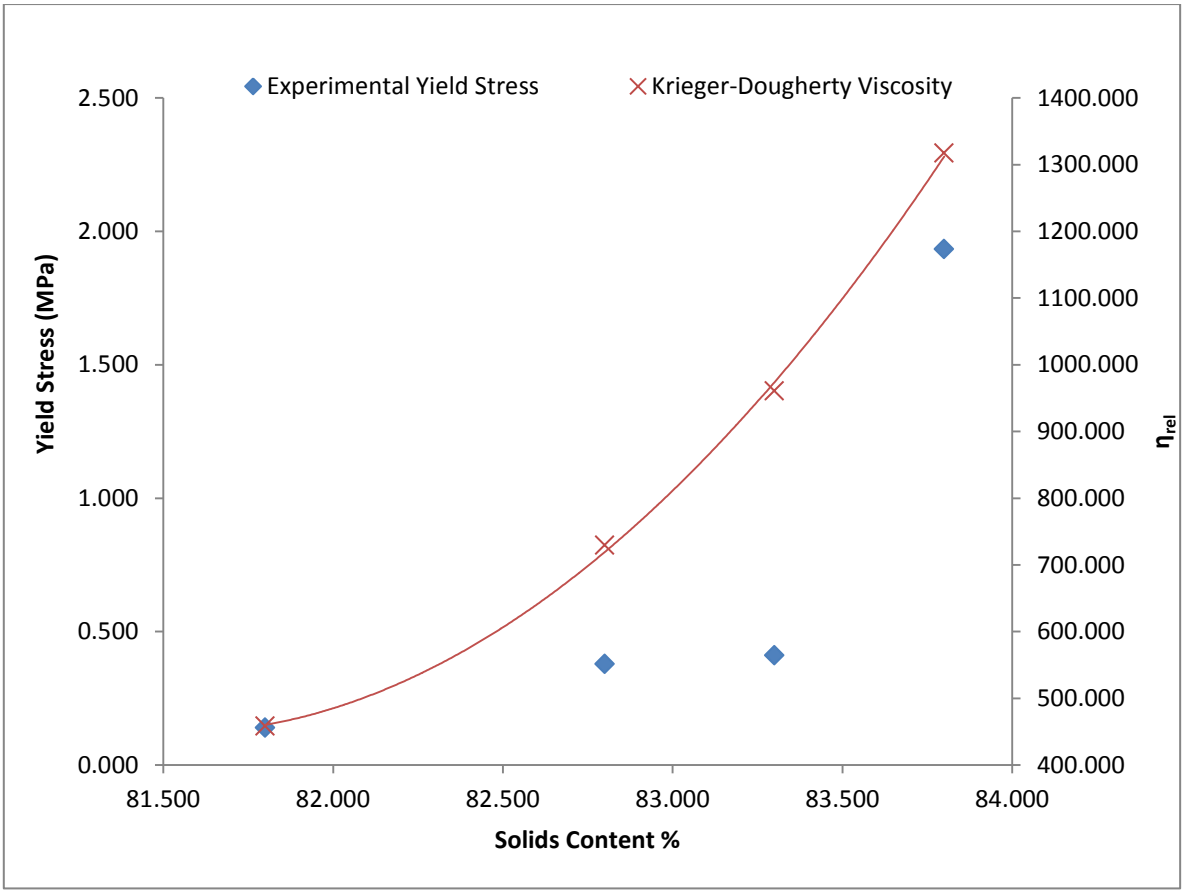

Figure 29 - Graph to show yield stress against solids content for the four pastes tested and Krieger-Dougherty plot (ϕ_m = 0.87)

Figure 29 shows the relationship between solids content and yield stress, showing an exponential increase as the maximum packing fraction is approached, and approaching a yield stress of zero when the solids content is low. The flat section of the experimental yield stress graph shows a similar trend to work previously done in the field [25] which attributes this plateau to slip flow behaviour; that is, the lubricating liquid layer near the wall is unaffected by the addition of more solids to a certain point.

7.2 Sodium Salt Selection

The pressure required to extrude the hollow tube is dependent on the rheology of the binder system as well as the amount of binder in the paste. The binder consists mostly of hydroxypropyl methylcellulose (HPMC) and polyethylene glycol (PEG) in deionised water. Many sodium salts are soluble in water, and as such may interact with the binder system and change its rheology.

Four different sodium salts were tested; oxalate, aluminate, acetate and bicarbonate. Sodium oxalate was included in the original formulation [26] and investigation during small scale extrusion showed that it gave a smooth extrudate suitable for the production of closed end tubes. These experiments were designed to investigate whether other sodium salts could perform as well, or possibly better, giving less pressure fluctuation or a lower extrusion pressure. Although, not a part of this study, the choice of sodium salt could also affect the sintering stage, with more soluble sodium salts likely to be more evenly distributed after drying. Sodium salts where added so that the molar aluminium: sodium ratio was kept constant while keeping the alumina content the same at 5.83 moles of aluminium per mole of sodium.

7.2.1 Sodium Bicarbonate

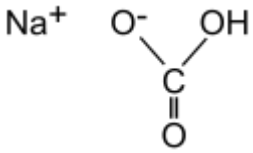

$NaHCO_3$

M_r = 84g/mol [27]

Solubility = 96g/litre

Density = 2.2g/cm^3

Addition of sodium bicarbonate resulted in the paste turning into a solid when left overnight, even at low concentrations of the sodium salt. Samples were set up with increasing concentrations of sodium bicarbonate, and were found to set in order of decreasing concentration, with the highest

concentration solidifying the most rapidly. It was found that the bicarbonate reacted with the HPMC in the binder system, and as such this salt was disregarded [20].

7.2.2 Sodium Aluminate

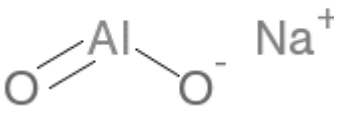

$NaAlO_2$ or $Na_2 Al_2 O_4$ or $NaO.Al_2O_3$

M_r = 81.97g/mol

Solubility = 509g/litre

Density = 1.5g/cm^3

Sodium aluminate was added to the paste, with care being taken to maintain the aluminium: sodium ratio. This was especially important in this case as the sodium compound contains aluminium atoms, with alumina being formed when the salt is added to water. As a result of this, only 250.75 g of alumina were added, with 81.65 g of sodium aluminate.

As the solubility of this salt is different to that of sodium oxalate, water was slowly added during the mixing process until the mixture was observed to form a paste. This point is easily identifiable by the absence of powder in the mixing vessel, given enough time between additions of water. This paste required 55 g of deionised water to form a paste.

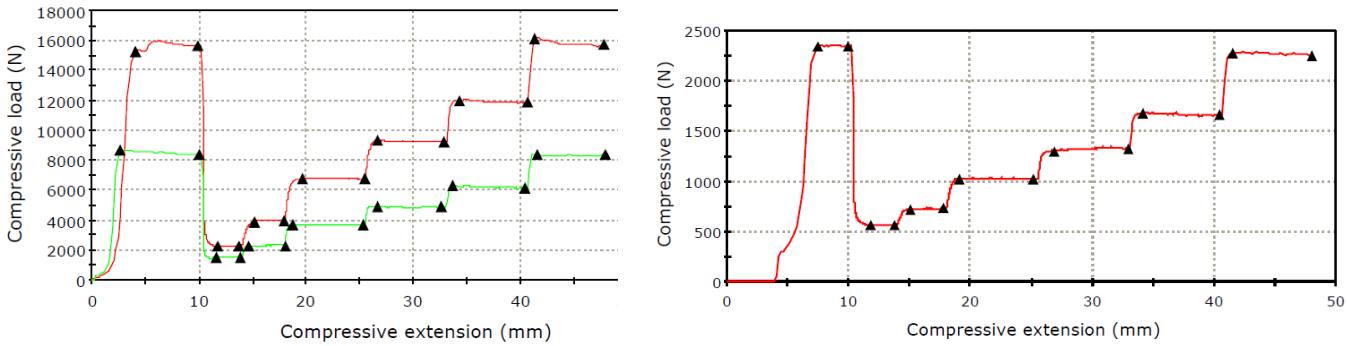

Figure 30 - Graphs to show pressure against extension for sodium aluminate, with L/D = 16 (left, upper), 8 (left, lower) and 1 (right)

Figure 30 shows the results from the small scale extrusion test of sodium aluminate. The highest observed pressure was around 16 kN, which was much higher than that observed for sodium oxalate (see Figure 27). This paste contained less water, however, and therefore this would be expected. The

results from the test show the pressure stays constant at each velocity, in contrast to the result obtained for the oxalate paste, despite containing less water. This suggests that air bubbles in the barrel were much more easily removed for this paste. There is also little difference between the two pressure readings at 50 mm/min, the first and last sections in each test. This suggests a lack of phase migration during the process, a highly desirable characteristic.

The fact that less water was added to this paste is a redundant fact without considering the solubility of the sodium salt. In this case, the solubility is much higher than that of oxalate, which reduces the solid mass fraction with respect to the liquid fraction. As a result of this, the paste is less densely packed for the same mass of water added.

Despite the data suggesting that sodium aluminate is a good choice for the production of closed end tubes, it was also necessary to consider the extrudate itself. It was observed that the extrudate suffered from regular surface fractures at higher velocities, with a build-up of material around the die exit. Surface fracture was only present in ram velocities above 2mm/min, giving an extrudate velocity of 140mm/min. This is unsuitable for the production of BASE tubes, as their surface should be smooth. When drying, the wet ceramic must be able to hang from the die, and the surface fractures would be a weak point for the tube to tear away.

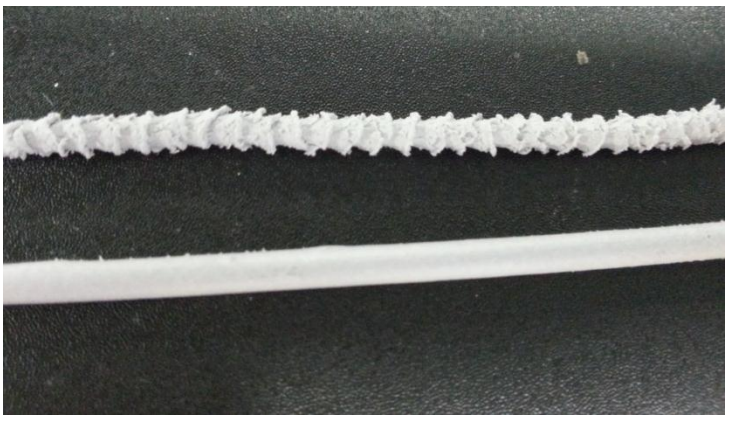

Figure 31 - Sodium aluminate paste extrudate, extruded at ram speeds of 50mm/min (top) and 1mm/min (bottom) (Diameter = 3mm)

7.2.3 Sodium Acetate

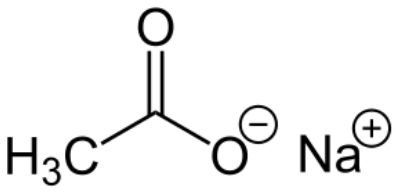

CH_3COONa

M_r = 82.03g

Solubility = 464g/litre

Density = 1.528g/cm^3

Sodium acetate was also considered as a source of sodium ions in the BASE tube. As with aluminate, the formula for 16.7% moisture was taken, only this time the α-alumina content was kept the same. Water was slowly added while mixing to ensure that the lower end of the window of operation for extrusion was found. For this paste, it took several hours of mixing and water addition before no powder was present, by which time 90 g of deionised water had been added, significantly higher than the previous pastes. Additionally the paste was observed to stick strongly to metallic surfaces, which would prevent the formation of a closed end using the extrusion method.

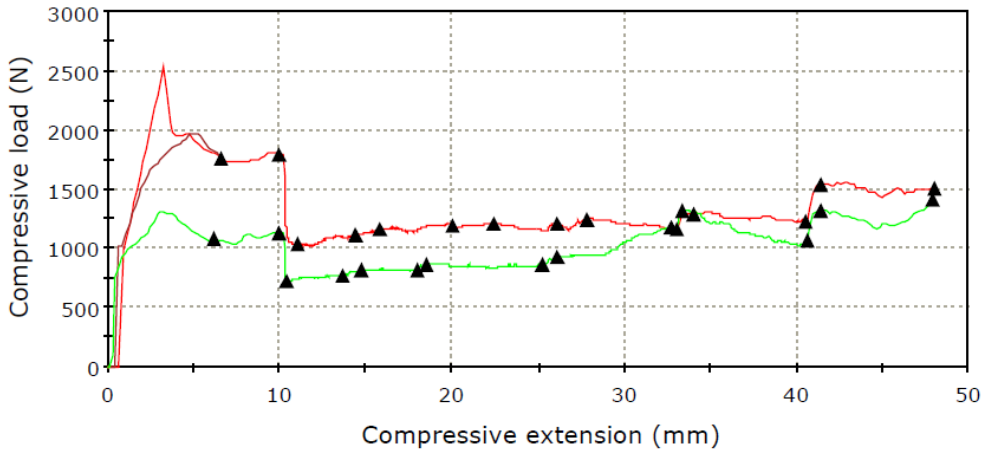

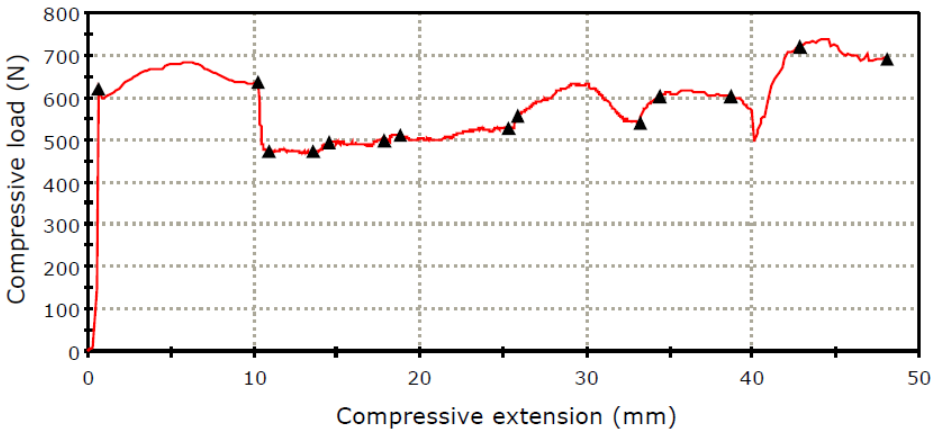

Figure 32 - Graph to show pressure against extension for sodium acetate pastes for L/D values of 16 (top, red), 8 (top, green) and 1 (bottom)

Figure 32 shows the results from small scale extrusion tests of the paste containing sodium acetate. It can be immediately observed from the graphs that the pressure fluctuated much more for this paste than any of the other formulations tested. Additionally, there is a poor correlation between velocity and pressure for ram velocities between 1 mm/min and 20 mm/min, particularly when compared to the smooth data from the aluminate paste. The fact that the mixing vessel was extremely difficult to clean after sample preparation also raises doubts over whether sodium acetate is a feasible compound for use in the industrial production of BASE tubes.

Such a weak relationship between pressure and velocity suggests that the paste behaves similarly to a perfect plastic, a material which shows pressure is independent of velocity. HPMC in the binder should ensure that the paste is a shear thinning material, however the paste showed little cohesion and stuck to metallic surfaces. A higher pressure requirement at the final speed of 50 mm/min compared to the initial section at this velocity suggests problems with phase migration in the paste.

To investigate this further, three representative binder solutions were prepared for rheological analysis, containing 40 g of near boiling water and 2.5 g of HPMC. To a second beaker, 12 g of sodium acetate was added, a value far below the saturation amount, and to the third, 1 g of sodium oxalate was added, also below the saturation point. All three samples were thoroughly stirred using

a spatula, before being covered in cling film and left overnight. It was observed that while the pure HPMC solution produced a clear gel, the sodium acetate beaker contained a clear liquid with two separate solid phases, which could be stirred into a suspension which settled after a period of time. The sodium oxalate beaker contained a bottom layer similar to the pure HPMC beaker, with a clear liquid on top. It was intended to test all three substances in a parallel plate rheometer, however when attempting to homogenise the sodium oxalate mixture, large amounts of air became entrapped in the thick gel, making it unsuitable for accurately obtaining rheological properties due to a lack of homogeneity. It was possible to perform rheometry on the other two solutions, the results of which are shown in Figure 33.

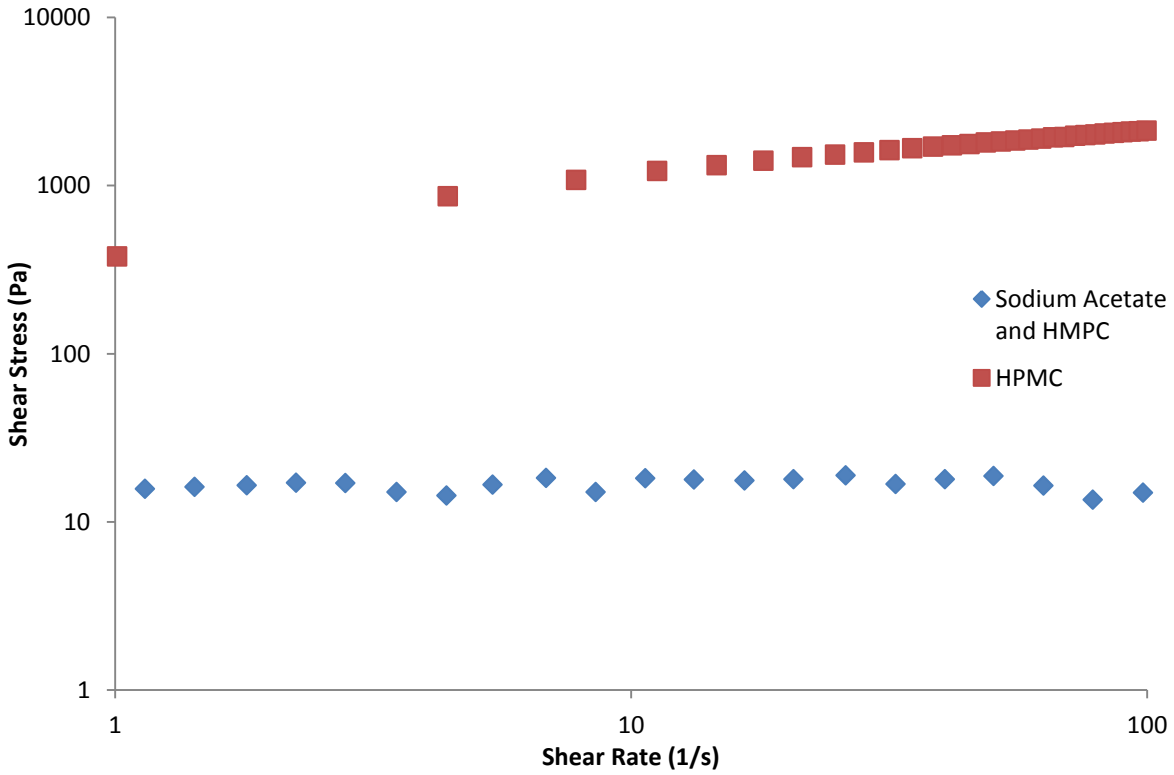

Figure 33 - Logarithmic plot to show rheological behaviour of HPMC and sodium acetate

Figure 33 shows that the addition of sodium acetate significantly reduces the viscosity of the HPMC solution. Observations showed that the two solid fractions were very different in that one sank to the bottom of the beaker, while the other floated, shown in Figure 34. The presence of two insoluble solids suggests a reaction occurs between sodium acetate and HPMC, causing two products which

need further analysis to determine what exactly they are. The very low viscosity of this sample suggests that there is little, if any, HPMC in the liquid, which implies that most of the HPMC added reacts to form the insoluble solids observed.

Figure 34 - Photograph of sodium aluminate and HPMC mixture

Figure 33 also shows that, for the sodium acetate sample, increasing the shear rate has almost no effect on shear stress, with the graph giving a horizontal line. This goes some way to explaining the poor relationship between applied pressure and velocity, and illustrates the profound effect of the liquid phase on paste behaviour in extrusion even at a very high solids content.

7.2.4 Comparison of Sodium Salts

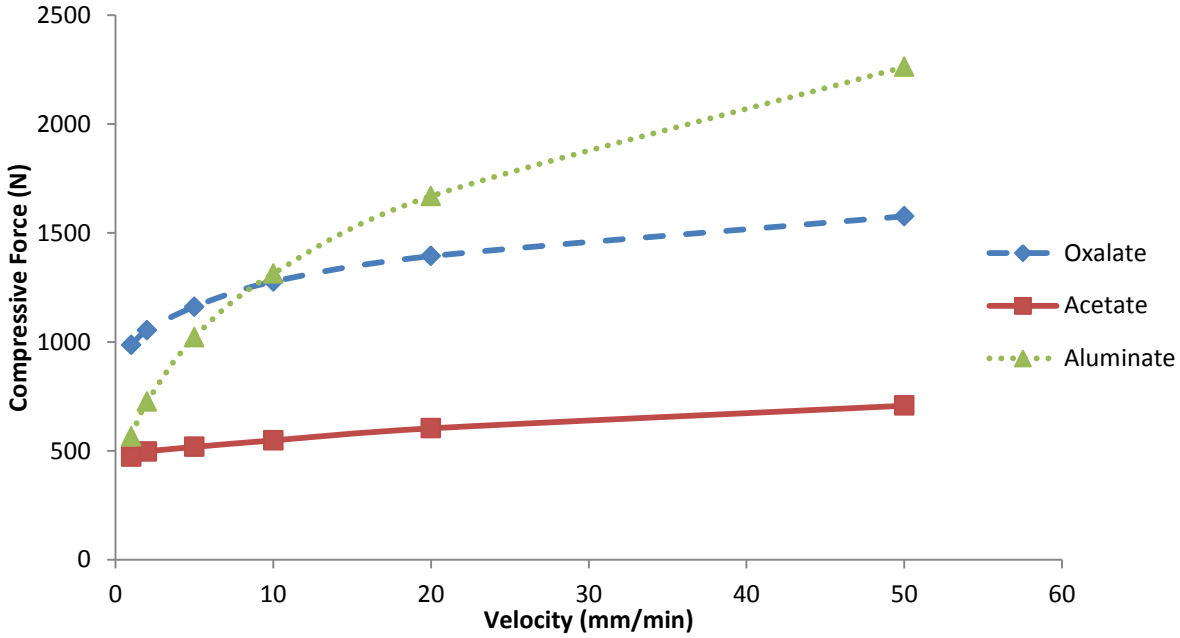

Figure 35 - Graph to show compressive force against ram velocity for the three different pastes mixed

Of the 4 sodium salts tested, sodium bicarbonate and sodium acetate were found to be unsuitable for use in the production of BASE tubes. Sodium aluminate showed promise, but the surface

fractures in the extrudate limit it to low ram velocities. When scaled up to an industrial scale, this may be an unacceptable factor in the production. Sodium oxalate exhibited lower extrusion pressures at higher velocities when compared to sodium aluminate, which gives it an advantage in mass production. It also produces a smooth, strong extrudate, making it the best choice of the salts tested.

It is worth noting that sodium oxalate has the lowest solubility of the sodium salts used, at 37 g/litre. It is energetically favourable for reactions to occur in the aqueous phase, and as such, very soluble sodium compounds are at risk of reacting with components in the binder system, changing the rheology of the paste.

7.3 Predictive Modelling

Once a paste had been characterised using the Benbow-Bridgwater parameters, the method outlined in the "Extrusion Modelling" section was used to predict the pressure required for the extrusion of the BASE tube. The Instron used to produce the tube gave a plot of pressure against ram displacement, similar to the graphs produced in small scale extrusion. Calculating the volume of each section, along with the pressure drop allowed the prediction to be superimposed on the actual experimental data to test the validity of the prediction.

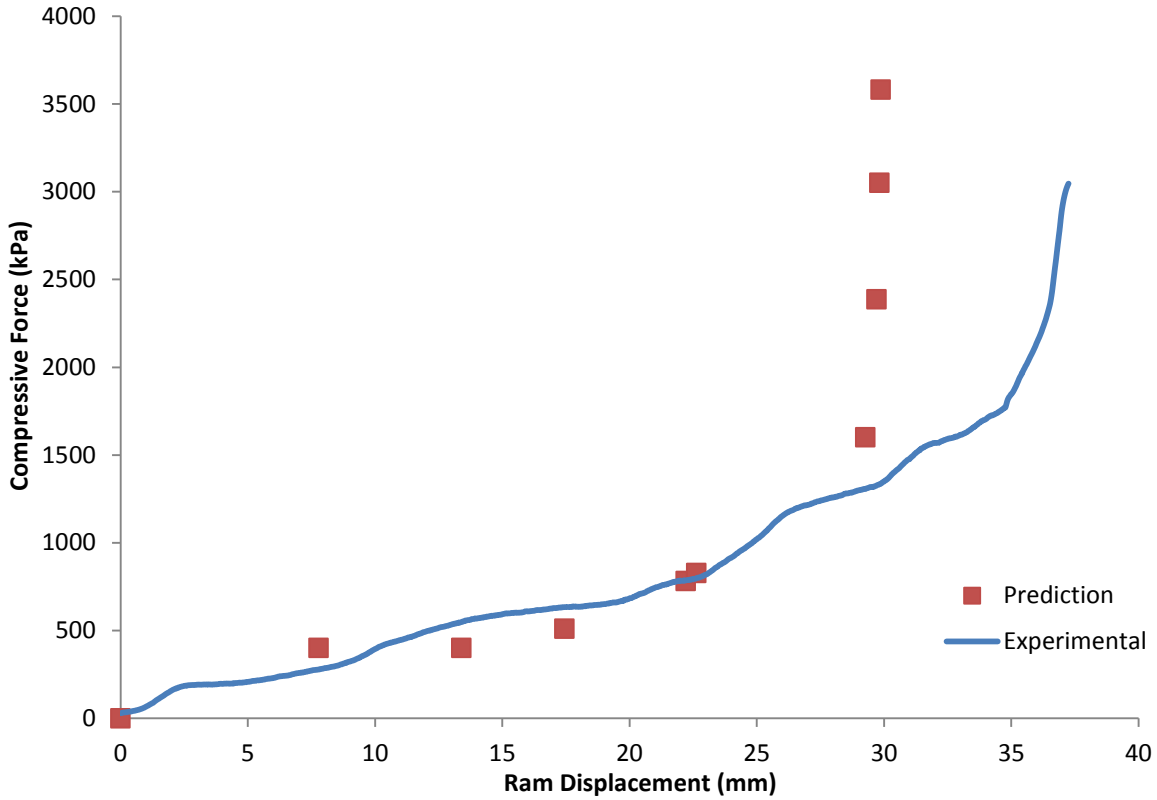

Figure 36 - Plot of pressure against ram displacement for 16.7% liquid content paste with model prediction

Figure 36 shows the extrusion profile of the 16.7% binder content paste, extruded at 4 mm/minute until the die was completely full. The prediction from the model is shown on the same graph. It is immediately clear that the model predicts that paste will emerge earlier than in the experiment. It does, however, show that the model predicted the maximum pressure required to within 15% of the actual value, and it is preferable that the actual pressure be less than the predicted pressure, where a higher experimental pressure than expected could damage the apparatus.

The inconsistency between actual and predicted ram displacement required could be attributed to incorrect assumptions in the model. It was assumed that the paste was incompressible. The ram displacement is out by around 7 mm for this experiment, which, assuming the work done through the 7 mm movement is used solely to compress to paste, gives a volume decrease of 1.33×10^{-5} m^3, while the paste is filled with around 1.9×10^{-4} m^3 of paste. Another assumption of the model was that the paste was perfectly packed into the barrel. The process of removing air bubbles from the

paste did not have quantifiable results, with just a mallet and a ram used. Indeed, a volume of 13.3cm^3 of air bubbles in the barrel would be unnoticeable. Even measuring the height of paste in the barrel would not help, as the volume varies depending on how much paste is removed from the mixer.

Correcting the model for the shortfall in volume is not easily done, as it is not obvious during which section the air bubbles are forced out of the barrel. It appears that the model fits the experimental data reasonably well until the paste enters the closed end section. It may be that at the pressures required to push the paste through the narrow channels inside the closed end cap, the air bubbles in the barrel escape through the ram end of the barrel, or the paste begins to become more dense. Transposing the final 3 points to the right by 7mm gives a much better correlation to the experimental results.

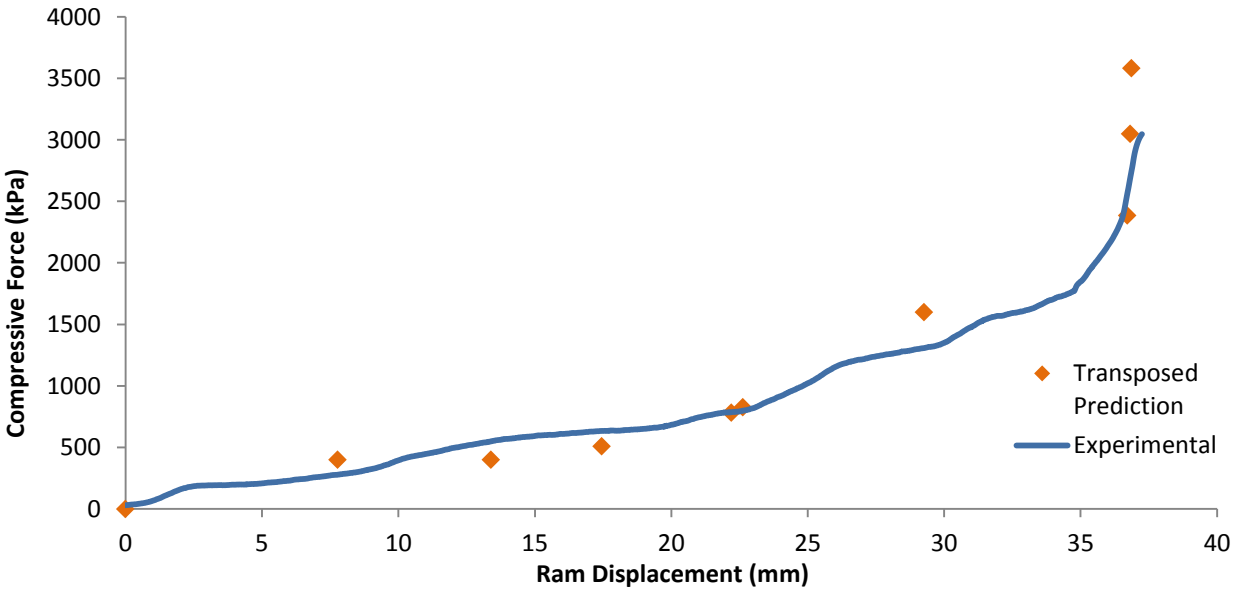

Figure 37 - Transposed prediction of pressure drop to neglect inaccuracies in ram displacement predictions

The experiment was always stopped as soon as paste was observed at the small outlet of the closed end cap, so as to not expose the die or stand to such high pressures for any longer than necessary. However the experimental data shows that the pressure may still be increasing at this point, implying that the emergence of paste from the end does not indicate steady state.

In order to gain a large amount of consistent material to carry out further tests, modelling dough was used to determine if, given sufficient time, the experimental pressure would eventually reach the predicted value. Due to the design of the die, it was possible to test this for the first stage alone by only assembling the first two pieces of the die to give just the barrel and spider. Due to how the die is designed, the only other way to partially assemble the die is with the closed end cap absent, producing a straight tube. This assembly was also tested with modelling dough to verify whether the inaccuracies of the model could be solely attributed to the increase in pressure associated with the thin channels in the formation of the closed end.

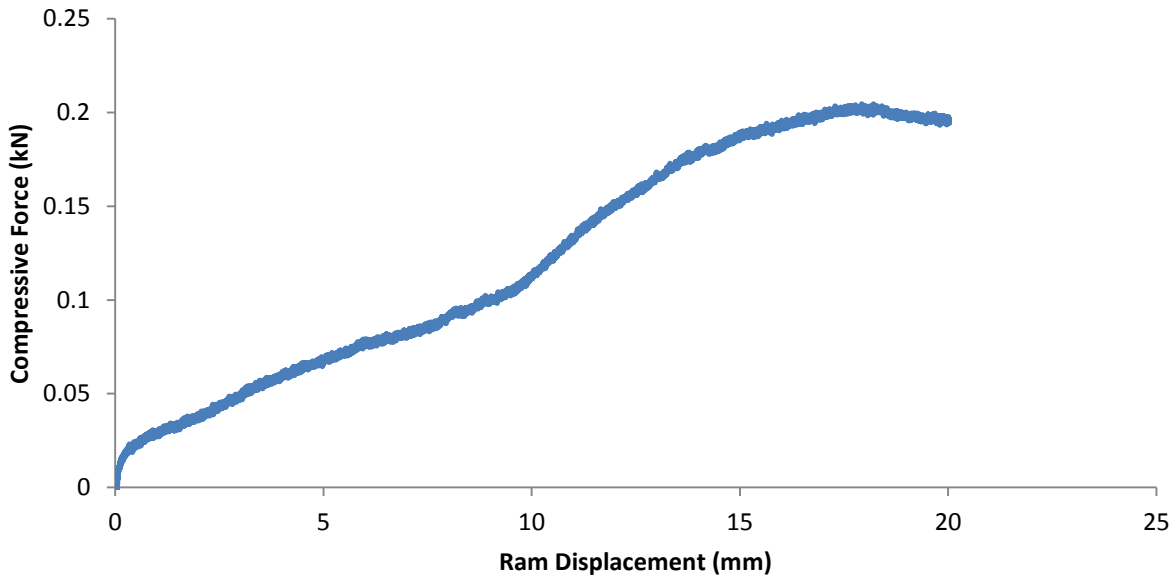

Figure 38 - Output from Bluehill software for model dough extruded through spider at 1 mm/min

Through small scale extrusion, the six Benbow-Bridgwater parameters were obtained, and the results are shown in Table 5 - Benbow Bridgwater Parameters of Modelling Dough below.

Table 5 - Benbow Bridgwater Parameters of Modelling Dough

Paramater	Value
σ (MPa)	0
α (MPa.s.m^{-1})	0.3512
τ (MPa)	0
β (MPa.s.m^{-1})	0.1533
m	0.3017
n	0.3153

Figure 38 shows the extrusion profile for model dough through the spider only, where the black triangle indicates the maximum applied pressure, with a value of 0.1975 kN. The model predicts a pressure drop of 0.242 kN, which is a large error at 22.5% larger than the actual value. Another interesting aspect of this graph is the change in gradient after a ram displacement of 9 mm. The volume of the spider is such that the ram should only have to move 7.78 mm for paste to emerge from the holes. It was observed that the paste emerged in the experiment after the ram had moved by around 16.5 mm, varying based on the extrudate not having a flat surface. Model dough is a much softer material than any of the pastes used in the die, and the fact that the distance the ram moves between the sudden gradient change, and the paste emerging is almost exactly what was predicted could suggest the initial 9 mm of movement forces much of the air in the barrel out, or that the dough compresses in this time. Additionally, the pressure was seen to continue to increase after paste emerged from the spider, though not to the extent that the model predicted.

The next piece of the die was added, and the velocity increased to 4 mm/min. Production of a hollow tube was carried out until a steady pressure was observed.

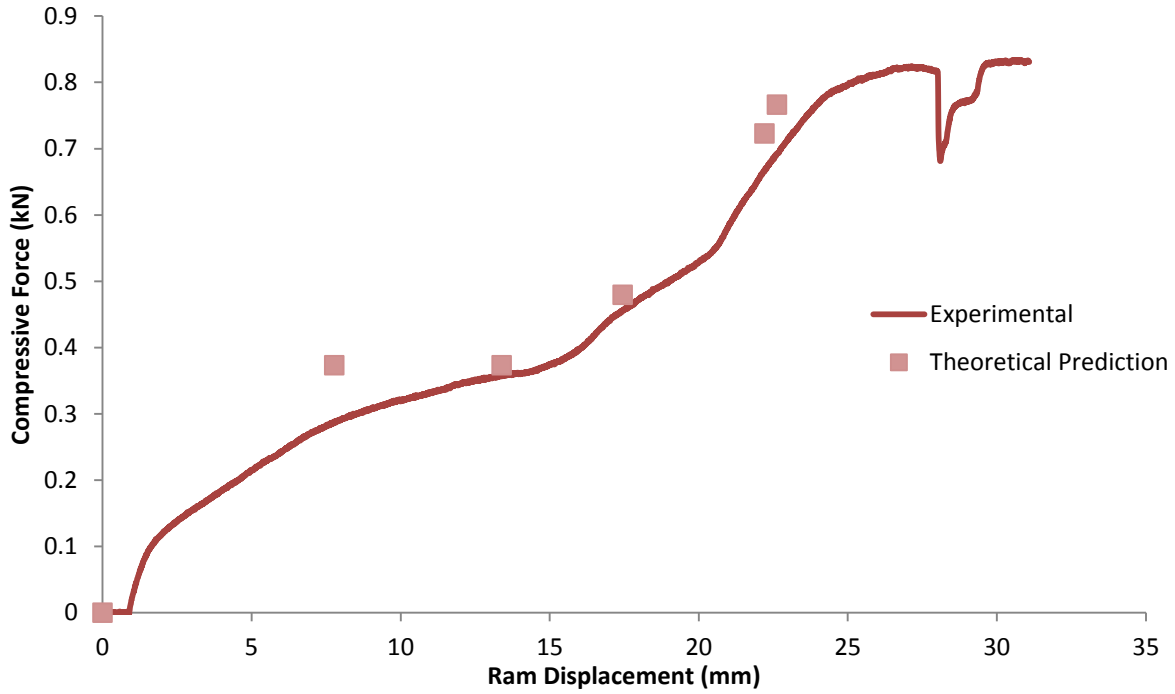

Figure 39 - Extrusion profile for model dough and theoretical prediction

Figure 39 shows the results of the experiment and the theoretical prediction made by the model. This graph shows that the model predicts the experimental pressure drop more accurately than in Figure 38 and Figure 36. However, the prediction for the pressure drop through section 1 is still much higher than the experimental value, and is only corrected by the fact that the cross sectional area then increases, giving a calculated pressure drop of zero. The experimental data shows that this is not the case, but the overall pressure drop for the two sections is similar in both the experiment and prediction. Additionally, the predicted and actual values of ram displacement are much closer in this experiment than in any of the previous results. This could be due to the barrel not being refilled between the results in Figure 38 and Figure 39, meaning all the suspected compression and air removal in the barrel was not a factor, resulting in the assumptions made in the modelling to be more valid in this case. The large pressure decrease observed after steady state is first reached suggests a large amount of air being released. This could be air present in the static zones where the barrel meets the first die land, which became trapped while cleaning out the spider between experiments.

7.4 Extrusion of Tubes

The extrusion of BASE tubes was performed with mixed success. The formation of the closed end was found to be easier with pastes that didn't stick to the PTFE cap, such as the 16.7% binder paste. However, cracks seemed to form during the drying process as the ceramic shrinks away from the PTFE.

Figure 40 - Photo of cracks in closed end tube (D = 0.05m)

Figure 40 shows the cracks observed in a dried tube. As the wax is still inside the tube after being released before further extrusion, the inside wall of the closed end cannot undergo shrinkage during drying to the same extent as the outer wall. The inside wall also dries more slowly due the wall being in contact with wax rather than air. These two effects culminate in the outer wall cracking to make up for the difference in rate of shrinkage.

One of the most challenging aspects of producing BASE tubes through extrusion is obtaining a straight tube. A slight misalignment between the centre pin and the outer walls of the die would cause the distance between the two to vary around the circumference. This caused a difference in linear velocity of the extrudate, causing the extruded tube to become curved. The Na-S battery requires a straight BASE tube, and so efforts were made to prevent misalignment.

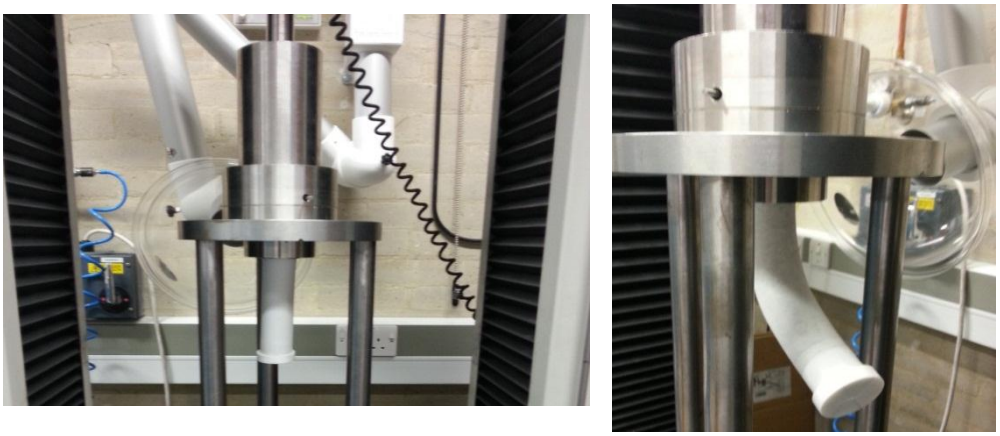

Figure 41 - Straight tube during extrusion (left) and the more commonly seen curved tube (right)

A brass tube with the same thickness as the BASE tube to be extruded was used to ensure the central pin and outer wall were aligned during assembly of the die and attaching the wax seal. It was inserted into the die exit before tightening the screws that held the die together were tightened. Despite this, the problem persisted, it was concluded that high pressures in the extrusion process could be causing the central pin to become misaligned again, regardless of measures taken during die assembly. The screws that keep the tube exit piece attached to the barrel and piece containing the spider were made larger, in an attempt to reduce movement between the two during operation.

This modification appeared promising, as the curvature of the extrudate was less severe, and use of the small screws in the sides of the tube outlet allowed any misalignments to be corrected during operation. The problem with this, was that by the time the curved extrudate had been observed and corrected, the tube must have already been extruded a significant length in order for the operator to recognise which screws to turn to correct the tilting.

In the modelling dough experiment, it was demonstrated that a “pre-compression” of the paste in the barrel before extrusion could lead to more consistent ram displacement values, as there are difficulties in loading the paste in a way which gives the barrel contents uniform density.

Variations in paste formulation caused by moisture loss meant some pastes had a lower total extrusion pressure than others. It appeared that a lower extrusion pressure gave rise to a straighter tube, which led to successful production; however, once a tube has been produced, it must be left hanging from the die to dry before being cut off. Pastes that require a low extrusion pressure were observed to not have a high enough green strength to remain suspended. Adding support to the drying ceramic also proved unsuccessful, as while drying, the ceramic shrinks and loses contact with support from underneath.

The result is disappointing, as such a high failure rate makes the method unsuitable for industrial use in its current form. The one success, however, offers hope that the method may be adapted to be made more consistent. It has been shown [3] that variation in the die land length is the cause of curved extrudates, therefore redesigning the die to ensure that assembling the many parts resulted in the same dimensions every time may yet prove this method a viable replacement to electophoretic deposition.

8. Conclusions and Further Work

From the experimental work presented in this thesis, the following conclusions can be drawn;

- When extruding hollow structures, the optimum binder content lies in the upper end of the "window of operation", where the yield stress is just below that which would be too stiff to extrude
- For this particular, application, a binder content of 16.7% was the most suitable.
- Sodium salts with a lower solubility are desirable as they are less likely to interact with chemical species in the binder, changing the rheology of the paste.
- It is possible to accurately predict the pressure required to extrude a paste for complex die geometries
- It is difficult to predict when extrudate will emerge from a complex die due to pockets of air in the barrel and the resulting compressibility of the paste.

Further work should be carried out to determine exactly where the optimum binder content exists. Investigation into a wider range of sodium salts is required to establish a link between solubility and rheology. Using a wider range of sodium salts may identify a more desirable source of sodium ions. The binder content of the sodium aluminate paste could be altered to determine if surface fractures can be eliminated by making the paste stiffer or softer. Recent work by others has shown NaSICON ceramic membranes to have a higher conductivity than sodium beta-alumina.

A redesign of the die could include measures to ensure the alignment of the centre pin with respect to the die walls. Use of a strong transparent material in the making of some parts of the die could help identify the flow patterns in the expanding section of the die, as well as the origins of surface fracture for the sodium aluminate paste. Such techniques have already been proven to be possible in identifying the causes of surface fracture in different pastes [28]. Positron emission particle tracking (PEPT) could also be used to determine the position of the paste in the assembled die, which would aid the modelling step.

9. References

[1] International Energy Agency, *World Energy Outlook, Paris* 2012.

[2] X. Lu, G. Xia, J. P. Lemmon and Z. Yang, "Advanced Materials for Sodium-Beta Alumina Batteries: Status, Challenges and Perspectives," *Journal of Power Sources,* vol. 195, (2010) pp. 2431 - 2442,

[3] J. Benbow and J. Bridgwater, Paste Flow and Extrusion, Clarendon Press, Oxford, 1993, ISBN: 0198563388

[4] M. Adams, Lecture Script: "Introduction to Rheology," in *Department of Chemical Engineering*, University of Birmingham, 2012.

[5] R. Greenwood, Lecture Script:"Rheology of Suspensions," in *Department of Chemical Engineering*, University of Birmingham, 2012.

[6] E. Bingham, "An investigation of the Laws of Plastic Flow," *US Beureau of Standards Bulletin,* vol. 13 (1916) pp. 309-353,

[7] I. Krieger and T. Dougherty, "A mechanism for non-Newtonian flow in suspensions of rigid spheres," *Transactions of the Society of Rheoloy,* vol. 3 (1959), pp. 137 - 152

[8] S. Blackburn, Lecture Script: "Paste Extrusion," in *Department of Chemical Engineering*, University of Birmingham, 2012.

[9] D. Price and J. Reed, "Boundary Conditions in Electrical Porcelain Extrusion," *American Ceramic Society Bulletin,* vol. 62, issue 12 (1983), p1348 - 1350.

[10] G. Onoda, "The Rheology of Organic Binder Solutions," in *Ceramic Processing Before Firing*, Wiley, New York, 1978. ISBN: 0471654108

[11] P. Martin and D. Wilson, "Rheological study of a talc-based paste for extrusion-granulation," *Journal of the European Ceramic Society,* vol. 24, no. 10 – 11 (2004) pp. 3155 – 3168.

[12] A. Domanti and J. Bridgwater, "An investigation of fracture criteria for predicting surface fracture in paste extrusion," *International Journal of Mechanical Sciences,* vol. 44 (2002) pp. 1381 – 1410.

[13] A. Domanti and J. Bridgwater, "Surface Fracture in Asymmetirc Paste Extrusion," *Trans IChemE,* vol. 78, 2000.

[14] J. Sudworth and A. Tilley, The Sodium Sulfur Battery,: University Press, Cambridge, 1985. ISBN: 0 412164906

[15] R. Gordon and S. RW, "Method for preparing shaped, green ceramic compacts". United States of America Patent 4020134, 26 April 1977.

[16] R. Gordon, B. McEntire, M. Miller and A. Vikrar, “Processing and Characterization of Polycrystalline β”-Alumina Ceramic Electrolytes,” *Materials Science Research,* vol. 11 (1978) pp. 405 – 420.

[17] R. Collongues, D. Gourier and A. Kahn, “Beta Alumina, A Typical Solid Electrolyte,” *J. Phys. Chem. Solids,* vol. 45, no. 10 (1984), pp. 981-1013.

[18] A. Theodore, “Ultrasonic End Capping of Beta''-Alumina Tubes”. USA Patent 4364783, 21 December 1982.

[19] NGK Insulators, last accessed on 28/04/2013, retrieved from URL: http://www.ngk.co.jp/english/products/power/nas/principle/index.html 2013. [Online].

[20] M. Frohlich and P. Okoji, Undergraduate Final Year Research Project, “Influence of Salt Composition on Alumina for Energy Storage Application,” University of Birmingham, 2013.

[21] O. Draper and S. D. G. Blackburn, “A comparison of paste rheology and extrudate strength with respect to binder system and forming technique,” *Journal of Materials Processing Technology,* Vols. 92-93 (1999), pp. 141 - 146.

[22] L. Swain, *Benbow-Bridgwater Curve Fitting Program,* Personal communication, 24th January 2013.

[23] J. Powell, “The Development of a Process for the Manufacture of Multilayered Ceramic Microtubes,” Journal of the European Ceramic Society, vol. 29 (2009), pp.893-897

[24] R. Greenwood, Lecture Script: “*Rheology of Suspensions*”, University of Birmingham, 2012.

[25] J. Powell and S. Blackburn, “Design of Ceramic Paste Formulations for Co-Extrusion,” *Powder Technology,* vol. 245 (2013), pp. 21-27.

[26] S. Blackburn, *Sodium-Beta Alumina Formulation,* Personal Communication, 27th September 2012.

[27] R. Perry and D. Green, Perry's Chemical Engineer's Handbook, McGraw-Hill Professional, New York City, 2007. ISBN: 0071422943

[28] A. Domanti and J. Bridgwater, “On the Origins of Paste Fracture,” *Industrial and Engineering Chemistry Research,* vol. 43 (2004), no. 14, pp. 3750-3757.